UNIVERSITÀ POLITECNICA DELLE MARCHE

Master Degree in Biomedical Engineering

An innovative approach towards Orbital Trauma Reconstruction: Design of a medical device for repairing fractured orbital wall

Supervisor :

Dott. Ing. Marco Mandolini

Co-Supervisor :

Dott. Ing. Alida Mazzoli

Candidate :

Agostino Maiellaro

Academic Year 2019/2020

INDEX

LIST OF FIGURES

LIST OF TABLES

ABSTRACT

The orbits are two cavities located symmetrically on either side of the sagittal plane at the root of the nose and have a conical or four-sided pyramidal shape, which open into the midline of the face and point back into the head.

Each orbit consists of a base, an apex and four walls instead the boundaries of the orbit are formed by seven bones. The orbital wall and floor are common sites of facial bone fracture and may cause serious functional impairment.

The repair of orbital wall and floor fractures is difficult due to the complexity of the anatomical region involved, and the limited intraoperative view. Appropriate management of these injuries avoids diplopia, enopthalmos dystopia, and abnormal facial appearance.

During the past decades, autogenous bone grafts were considered ideal for the treatment of orbital floor fractures. Titanium mesh and high-density porous polyethylene implants are presently the most commonly used nonresorbable synthetic allopastic materials for orbital floor reconstructions, also are easier to handle and offer the possibility of obtaining a precise three-dimensional (3D) reconstruction.

The application of computer aided design and additive manufacturing for the production of patient-specific medical prostheses and implants, to reconstruct facial and orbital bones defects, has been described in several papers.

The aim of this study was to design a medical device capable of helping the surgeon to insert a titanium mesh prosthesis in a fractured eye socket, trying to highlight what could be the advantages and disadvantages compared to classical instruments used in surgery.

The first step to start the design and production process of the implant and the medical device was the acquisition of the scan images (CT) of the computed tomography (CT) first in the Mimics software and then in Rhinoceros v.6.29.

The mould and the medical device have been manufactured in polyamide using the Selective Laser Sintering technique (SLS).

The selective laser sintered mould is able to model and form several kinds of prosthetic materials, resulting in customised implants and allowing accurate orbital cavity reconstructions. Instead, the medical device proved that this procedure, at the same time, reduces the related costs, is sterilizable, usable in the operating room, easy to use and ergonomic.

A drawback is that it can only be used for titanium mesh implants, in fact the demineralized bone plate, highly used in surgery, cannot be used with this device. Several improvements may lead to an increase in accuracy at a later stage. The clinical feasibility should be evaluated in a future study as well.

INTRODUCTION

The orbital wall and floor are common sites of facial bone fracture and may cause serious functional impairment. The repair of orbital wall and floor fractures is difficult due to the complexity of the anatomical region involved, and the limited intraoperative view [1].

Fractures of the internal orbit can cause several problems, including ocular muscle entrapment limiting extrinsic eye movements, diplopia, enophthalmos, vertical displacements of the globe and loss in visual acuity.

The manual process for preparing implant is very labour intensive and expensive. Alternatively, it is possible to create custom made patient specific implants by using 3D modelling software and additive manufacturing (AM).

This process has potential for more accurate and cost-effective implants. Preoperative models are commonly used for planning or simulating difficult sections of surgical operations.

It is possible to design patient-specific implants digitally by using computed tomography (CT) images as a reference and by manufacturing the implant with traditional machining methods [2]. Different approaches based on anatomical or mathematical features of the eye-ball surface are available for the reconstruction of an orbital defect according to their size and shape: mirror-imaging of the unaffected side [3], thin plate spline surface interpolation [4] or anatomical reconstruction [5].

The aim of this study was to design a medical device capable of helping the surgeon to insert a titanium mesh prosthesis in a fractured eye socket, trying to highlight what could be the advantages and disadvantages compared to classical instruments used in surgery.

A brief overview of the bones of the eyeball in order to better understand and justify the choices that contribute to the definition of an adequate procedure to design the implant has been described. Moreover, a section is devoted to the presentation of the historical evolution of prosthetic implants and related materials.

Besides this, a review of the current techniques adopted in orbital cavity reconstruction field has been updated with the rapid prototyping technologies utilized in the fabrication of a solid 3D implant.

A computer-assisted approach, based on anatomical modelling, custom-made mould fabrication and design of a device for the insertion of the prosthesis in the fractured wall via selective laser sintering (SLS) is proposed.

Subsequently, all the flow that led to the design of the CAD models was defined. As regards the modeling of the implant, a specific workflow was defined which led to its realization.

Then, in accordance with the literature, clinical and mechanical requirements were defined for the realization of the mould. Regarding the medical device, in addition to the requirements, other characteristics were defined, such as functions, specifications and house of quality that allowed to

provide further information for the design. The device is also divided into two parts hinged together and has a spring capable of increasing the degree of ergonomics of the same, allowing the upper part of the device to close and properly grasp the prosthesis.

The first step to start the design and production process of the implant and the medical device was the acquisition of the scan images (CT) of the computed tomography (CT) first in the Mimics software and then in Rhinoceros v.6.29.

For the realization of the custom-made implant, the relative mould and then, the medical device, the fracture of the orbital floor was simulated.

After having designed the custom-made implant, the mould was made starting from the implant itself. Regarding the device, an attempt was made to fully satisfy all requirements. It features a gripping mechanism, is low cost, usable and usable in the operating room.

In this case study, the mould and the medical device were made of polyamide using the Selective Laser Sintering (SLS) technique as it offers advantages that satisfy the requirements described for their realization.

The result was obtained from the 3D printed fabrication of a mould involved in a pressure mechanism capable of modeling a titanium mesh, according to the previously designed implant. The titanium mesh modeled from the mould has been correctly taken by the medical device. Furthermore, to improve the effectiveness of the device, a spring has been added to make it more ergonomic and a hinge placed at the end of the device to better fix the two parts. The results show that the device fulfills most of the described requirements. It is easy to use, being made of polyamide by sls it is easily sterilized and can be used for fractures of the orbital floor. A drawback is that it can only be used for titanium mesh implants, in fact the demineralized bone plate, highly used in surgery, cannot be used with this device. Several improvements may lead to an increase in accuracy at a later stage. The clinical feasibility should be evaluated in a future study as well.

1- ORBITAL ANATOMY AND FRACTURES

1.1 Anatomical structure of the eye socket

The orbits are two cavities located symmetrically on either side of the sagittal plane at the root of the nose and have a conical or four-sided pyramidal shape, which open into the midline of the face and point back into the head [6]. Each orbit consists of a base, an apex and four walls (Fig. 1.1) instead the boundaries of the orbit are formed by seven bones.

The apex of the orbital pyramid is situated 44–50mm posteriorly and contains important neurovascular structures crammed into a very tight space.

The base of the pyramid is the orbital entrance, which is roughly rectangular, and it is known as orbital rim. The four walls are: Medial and lateral wall, Orbital roof, Floor [7].

The medial wall is roughly rectangular and extends from the anterior lacrimal crest (frontal process of the maxilla) to the orbital apex. Formed by the ethmoid, maxilla, lacrimal and sphenoid bones. The lateral wall, the thickest of the orbital walls, is formed by the greater wing of sphenoid posteriorly and the zygoma anteriorly. It is separated from the floor by the inferior orbital fissure and from the roof by the superior orbital fissure (posteriorly) and the frontosphenoid suture.

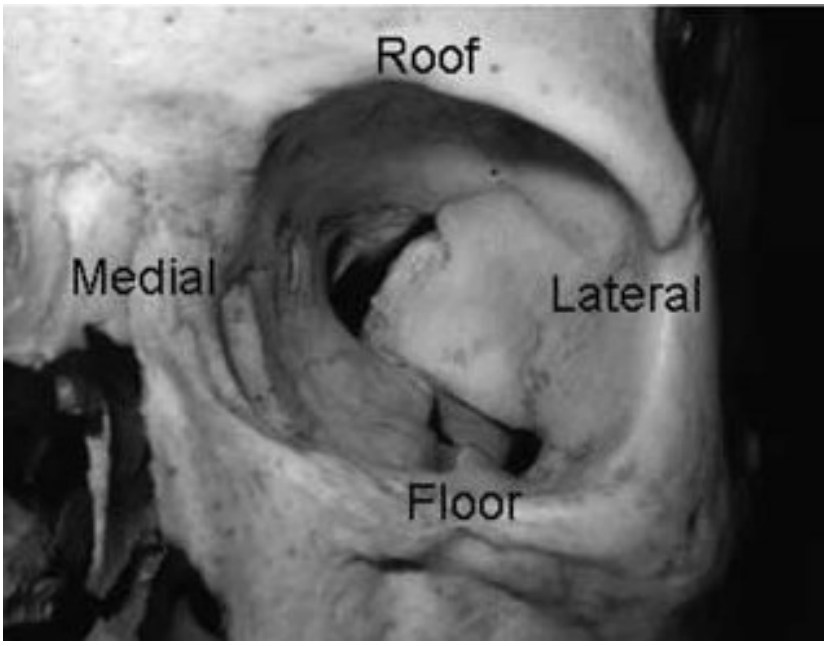

Figure 1.1: The bony orbit is pyramidal shape of the orbit. The base is situated anteriorly and the apex posteriorly.

The medial orbital walls also are parallel, approximately 2.5cm apart and separated by paired ethmoid sinuses. Each lateral wall forms a 45˚ angle with its respective medial wall, resulting in 90˚ between the two lateral walls (Fig. 1.2). The orbital volume is roughly 30 ml, of which 7 ml is occupied by the globe [7].

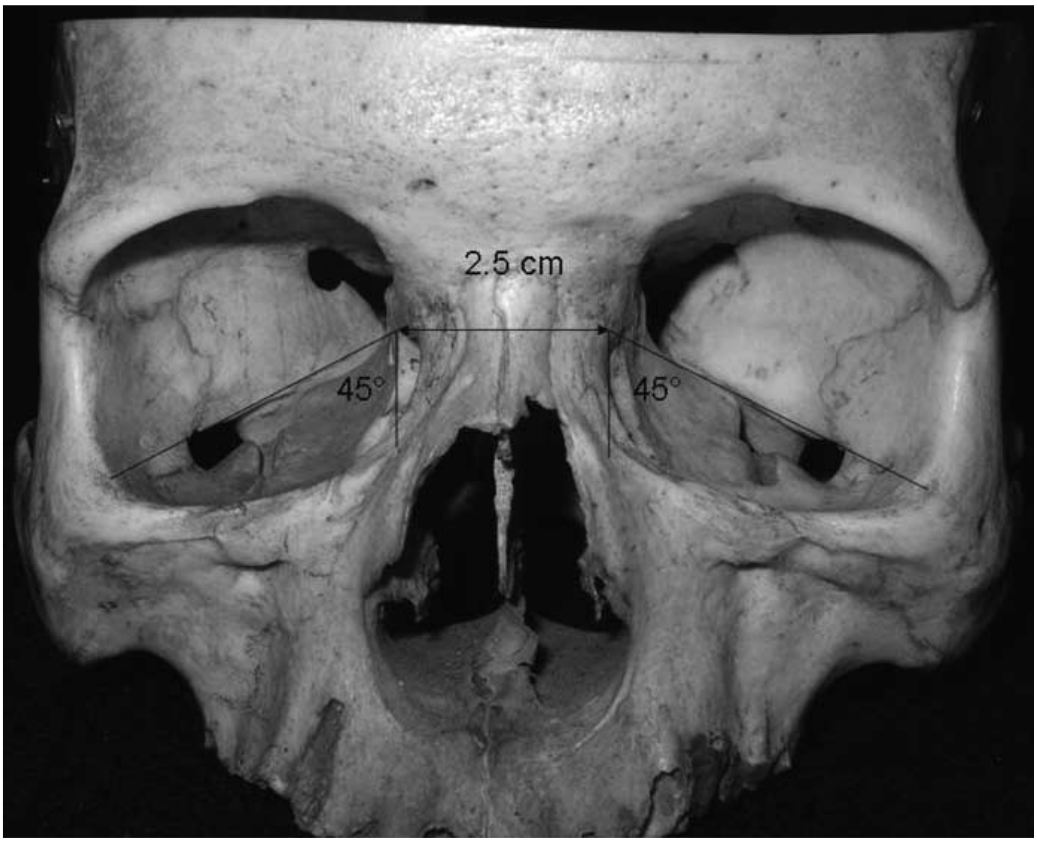

Figure 1.2: The relationship between the medial walls, the paired ethmoid sinuses, and the corresponding lateral walls.

Orbital roof is thin and concave in a downward direction. It can be separated into two laminae by the frontal sinus: there is the lacrimal fossa in the anterolateral part, and the anteromedial part houses the fovea into which the trochlea of the superior oblique muscle is inserted. The floor is triangular and slopes gradually upwards to merge almost imperceptibly with the medial wall at the maxilloethmoid suture. It is formed mainly by the orbital plate of the maxilla with contributions from the zygoma anterolaterally and the palatine bone at its most posterior limit (Fig. 1.3). Bone is the main supporting tissue of the body in terms of load bearing, despite it is a very lightweight material. Its composition includes protein (collagen about 90% to give flexibility) and mineral (crystals of hydroxyapatite impregnate the collagen matrix to make the structure stiffer) that can repair and reshape itself in response to external stresses.

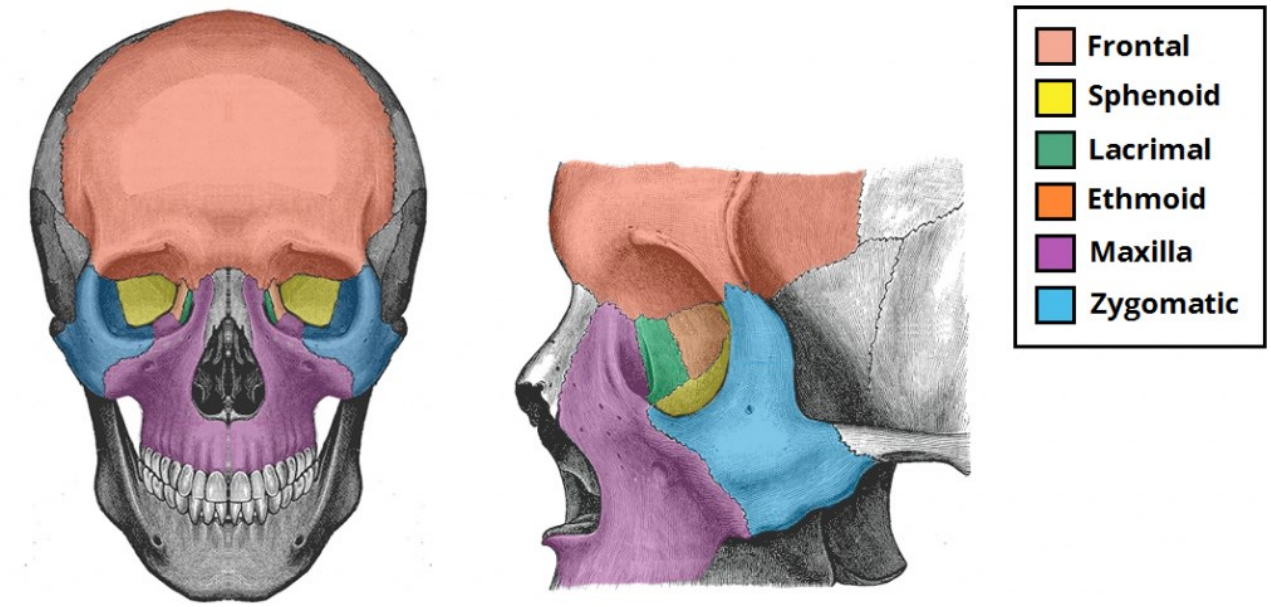

Figure 1.3: The anterior and lateral views of the bony orbit.

The orbit also can be split into two parts, an anterior part containing the eyeball and a posterior compartment containing the extra-ocular muscles, the vessels and the nerves supplying the eyeball, all supported in a cellular, fatty matrix, the so-called adipose body of the orbit (Fig. 1.4) [6]**.** The extra-ocular muscles are separate from the eye, are seven in which the first is the levator palpebrae superior muscle and the other six control the eye movements: four rectus muscles (superior, inferior, lateral and medial) and two oblique muscles (superior and inferior). Regarding the nerves, there are several types that supply the eye and its structure: optic, oculomotor, trochlear, trigeminal and abducens nerves. Instead, the eye receives blood primarily from the ophthalmic artery. Venous drainage is via the superior and inferior ophthalmic veins.

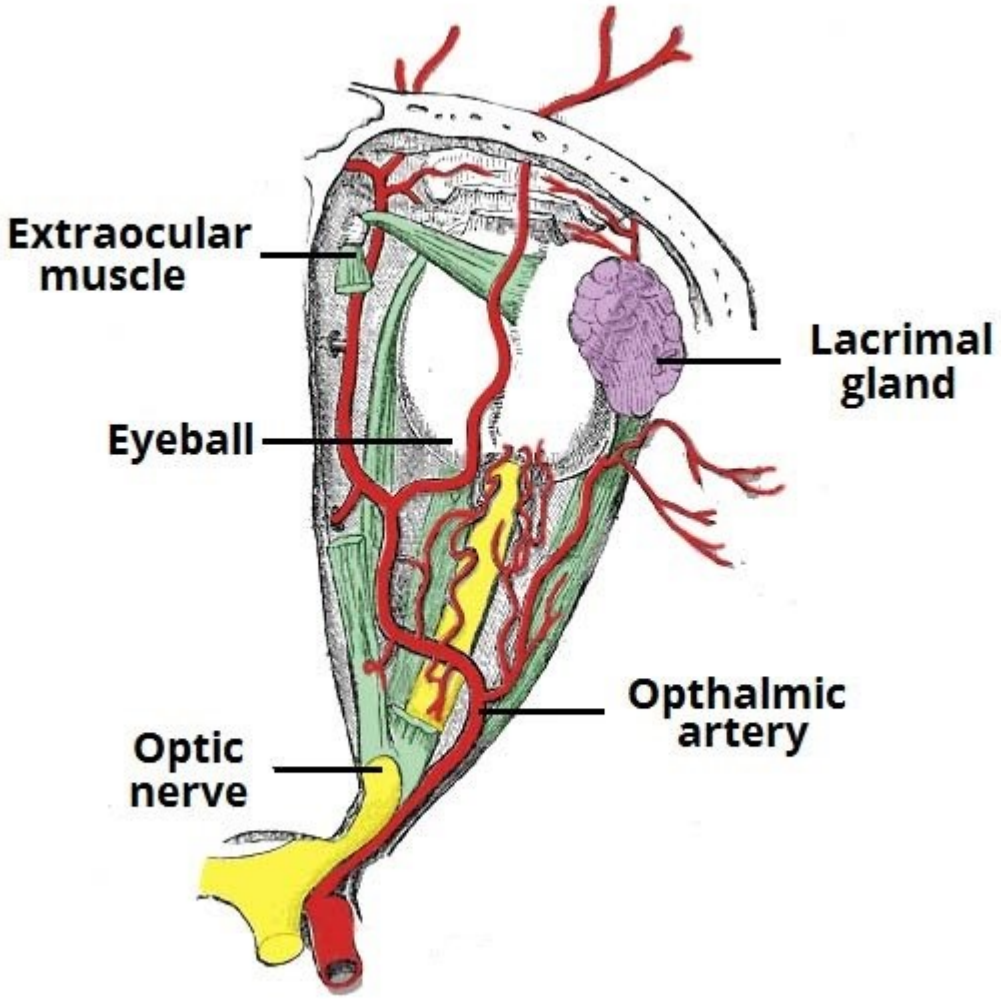

Figure 1.4: Representation of the bony orbit and their associated structures.

Structures can enter and leave the orbit through three different pathways: Optic canal, Superior orbital fissure and Inferior orbital fissure (Fig. 1.5).

The optic canal is a bony channel that connects the anterior cranial fossa and the orbit and contains the optic nerve and the ophthalmic artery. It is approximately 5 mm in diameter and runs in a superior medial direction into the cranial fossa. The canal itself is less than 1 cm in length and lies entirely within the sphenoid [8].

The Superior orbital fissure is a foramen at the back of the orbit that separates the orbital roof from the lateral wall of the orbit and connects the orbit to the cavernous sinus in the brain [9]. Located near the apex of the orbit lies a club-shaped fissure, where the greater and lesser wings of the sphenoid meet the maxilla. Transmits the lacrimal, frontal, trochlear, oculomotor, nasociliary and abducens nerves. It also carries the superior ophthalmic vein. Fractures, edema, or hematoma extending to the superior orbital fissure can result in ophthalmoplegia, ptosis, or pupillary dilatation [10]. The Inferior orbital fissure lies in the orbital floor in proximity to the superior orbital fissure, foramen rotundum, pterygopalatine fossa, infratemporal fossa, and temporal fossa. Transmits the zygomatic branch of the maxillary nerve, the inferior ophthalmic vein, and sympathetic nerves [11].

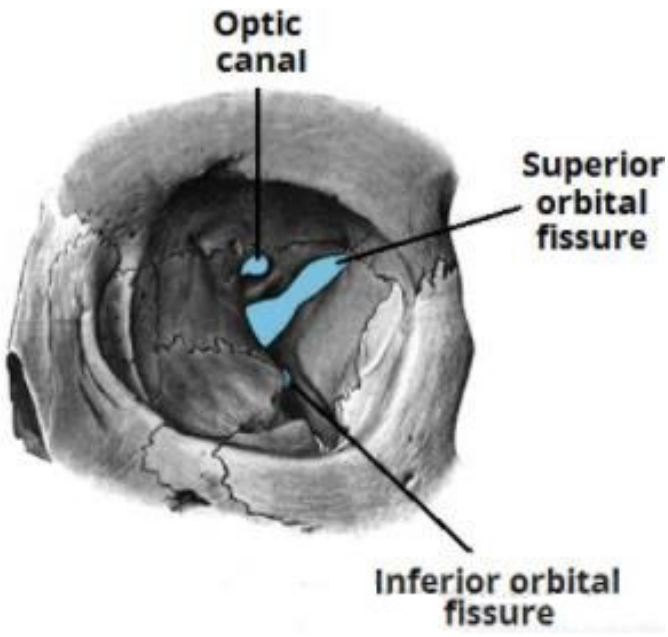

Figure 1.5: Pathways into the orbit.

1.2 Eye Socket Fracture

The eye socket is the bony structure surrounding and protecting the eye. In addition to the eye, it houses all the muscles, nerves, and connective tissues that connect to and move the eye. Some parts of the eye socket are hard, thick, and difficult to break.

Other areas are fragile and more prone to breaking. When one of the bones that forms this bony structure is broken it is called an orbital fracture. Orbital fractures are a consequence of middle third facial trauma and occur as a result of the application of forces that overcome the resistance of bone structures forming the orbital cavity.

These fractures are very frequently associated with damage to the surrounding soft tissue and they sometimes damage the orbital cavity contents or communicate the orbit with adjacent structures [12].

Fractures of the eye socket can be classified into the following categories: Orbital rim fracture, Blowout fractures, Orbital floor fracture.

The first one occurs in the outer edges of the eye socket. The orbital rim is very thick, so only extreme force, such as an injury from a car accident, can break it. This extra force can also injure the nerves, muscles, and connective tissues in the eye. The damage is usually in more than one area of the eye socket.

A common type of orbital rim fracture involves all three major parts of the eye socket. It's called a tripod fracture, or a zygomaticomaxillary complex (ZMC) fracture.

Blowout fracture of orbit involves fracture of orbital floor without fracture of infraorbital rim (Fig. 1.6). This type of fracture commonly happens when you are struck by something larger than the eye socket, such as a fist or blunt object.

The blowout happens when a punch or other blow to the eye causes a pressure buildup in the fluid of the eye. This pressure is transmitted to the eye socket, causing it to fracture outward.

Blowout fracture causes an increase in the intraorbital volume, this causes enopthalmos.

Entrapment of inferior rectus muscle causes diplopia. These patients usually report to an opthalmologist since orbital signs and symptoms are predominant [13].

The treatment of blowout fractures is a major challenge for the Maxillofacial surgeon and selection of the biomaterial is related to several factors, such as the size of the defect, the number of walls involved the adaptation of internal contours, restoration of appropriate volume, elapsed time of the trauma and the experience of the surgeon [14].

The orbital floor, which forms the roof of the maxillary sinus, slopes upward toward the apex of the pyramid, which lies roughly 44 to 50 mm posterior to the orbital entrance.

This complicated anatomy makes repair and reconstruction of orbital fracture difficult [15].

Orbital floor fractures may occur in isolation or as part of a zygomaticomaxillary complex fracture. This fracture can also affect the muscles and nerves around the eye, keeping it from moving properly and feeling normal. Orbital fractures are more common in males than in females and most often occur in men, ages 21 to 30 years of age [16].

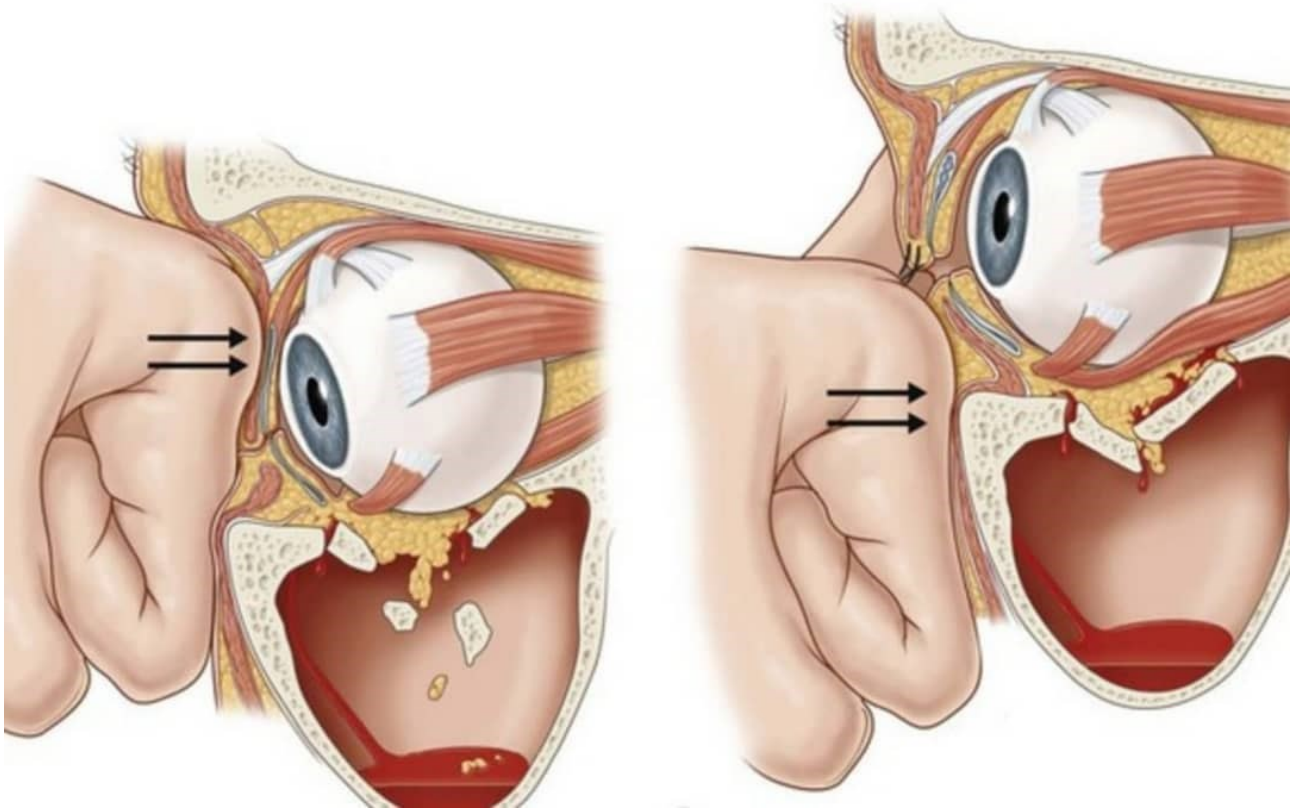

Figure 1.6: Mechanism of fracture of the orbital floor (blowout).

1.3 Symptoms of an eye socket fracture

Signs and symptoms are going to vary according to the cause and severity of the injury. Symptoms include [17] :

- Diplopia: injury result from swelling and bleeding into the tissue surrounding the eye or swelling and other injury that affect the muscles that control the eye movements;
- Limitation of upward gaze;
- Trigeminal function assessment: The infraorbital nerve runs along the floor of the orbit. decreased sensation over the inferior orbital rim, extending to the edge of the nose and ipsilateral upper lip;
- Tenderness, or step-offs at the infraorbital rim;
- Subcutaneous emphysema (indicates a fracture of the maxillary sinus);
- Oculomotor function: Entrapment of the inferior rectus muscle; often occurs between fragments of the lower orbit and is the cause of diplopia;
- Pupillary light reflex: An absent reflex can show damage to the afferent or efferent nerve system;
- Gross visual acuity;
- Position of the globe: A dislocated fracture can lead to enophthalmos and swelling be-hind the globe, to exophthalmos;
- Chemosis and sub-conjunctival haemorrhage;
- Edema and periorbital ecchymosis.

1.4 Treatment

Many clinicians have recommended that orbital volume increases be treated, as an indication for early reconstructive surgery. In general, surgery should be undertaken within 14 days to prevent fibrosis. Most surgeons wait 24-72 hours to allow the edema to subside before under-taking surgery. Patients with fractures where the orbital floor fragments are not displaced, and the orbital volume remains unchanged, can be addressed without any surgical intervention. In fact, the goal of surgery is to restore herniated structures into the orbital cavity. The surgery may be done via a transconjunctival or trans maxillary approach. Today there are endoscopic techniques to manage the orbital fracture. Several types of implants are also available for reconstruction of the orbit, but these should be avoided in the presence of an obvious infection.

2- ORBITAL SURGERY: LITERATURE REVIEW

The orbital wall and floor are common sites of facial bone fracture and may cause serious functional impairment. The repair of orbital wall and floor fractures is difficult due to the complexity of the anatomical region involved, and the limited intraoperative view [1].

Fractures resulting in orbital floor or wall defects larger than 10 mm in diameter, indicate the need for surgical treatment i.e open reduction, internal rigid fixation and orbital reconstruction [18]. Appropriate management of these injuries avoids diplopia, enopthalmos dystopia, and abnormal facial appearance [19].

During the past decades, autogenous bone grafts were considered ideal for the treatment of orbital floor fractures. However, it is important to consider the following factors: the quantity of bone required at the recipient site, the biologic qualities of the donor bone, the unpredictable resorption of the bone graft, and the considerable donor site morbidity.

These listed shortcomings associated with autogenous bone graft have led to the development of four basic types of implant materials for orbital wall reconstruction: allogeneic grafts, xenografts, nonresorbable synthetic alloplastic materials, and resorbable synthetic alloplastic materials [18]. Titanium mesh and high-density porous polyethylene implants are presently the most commonly used nonresorbable synthetic allopastic materials for orbital floor reconstructions, also are easier to handle and offer the possibility of obtaining a precise three-dimensional (3D) reconstruction [1]**.** Despite the large numbers of surgical techniques and implant materials, precise anatomical reconstruction of the orbital floor remains very challenging.

Limited visualization and the complex surface anatomy of the orbital cavity defy the surgeon's ability to accurately shape or place an implant to restore the pre-injury anatomy [20].

The use of high-resolution computed tomography (CT), with the ability to examine the scans routinely in three planes, has provided a better understanding of the three-dimensional (3D) structure of the bony orbit.

It should be taken into account that the management of orbital floor injuries is complicated by their technical difficulty. One of the most challenging aspects of orbital reconstruction is that the orbit is not a simple cone shaped structure. The three-dimensional (3D) structure of the orbit has complex concavities and convexities on the surface. Furthermore, the orbit of each patient has a different shape and volume.

The success of reconstructive orbital surgery depends on diverse aspects of the preoperative evaluation of the defect, the design and manufacturing of the implant and the execution of surgery [21]. In fact, prefabricated patient-specific implants, designed using a patient's computed tomography

(CT) data to precisely restore the missing anatomy, are increasing in popularity as a surgical solution for these more complex orbital defects.

These implants reduce surgical complexity, decrease operative times, minimize exposure and risk of contamination, and have resulted in improved cosmesis and patient satisfaction.

The fabrication of custom implants normally relies on preoperative processing of the patient's CT data, the computer-assisted design of a virtual implant model and subsequent manufacture of the implant [22].

Since their introduction in 1980, rapid prototyping techniques influenced more and more the biomedical field with different applications ranging from bio-printing tissues and organs to molds for prosthetics and surgical guides, patient-specific implant up to drug-delivery devices and forensic science [23].

The application of computer aided design and additive manufacturing for the production of patient-specific medical prostheses and implants, to reconstruct facial and orbital bones defects, has been described in several papers. Briefly, additive manufacturing (AM) techniques otherwise known as three-dimensional (3D) printing, refer to the process of building a device by joining material layer by layer.

Conversely to the traditional process of subtractive manufacturing, it starts from a computer-aided drafting (CAD) model decomposed into transversal sectional layers where virtual trajectories instruct the 3D 'printer' where to deposit the layers of material through proper technologies such as: Selective Laser Sintering (SLS), Fused Deposition Modeling, Multi-Jet Modeling and Stereolithography (STL).

Five technical steps are required to finalize a printed model. (Fig. 2.1) [24] .Generally speaking, the potentials of AM span over different fields and entail a reduction in the time to market, reduction of cost development, customization of unique item and spare parts, on-site and on-demand manufacturing, quality improvement, smaller environmental footprint as only needed materials are used [25].

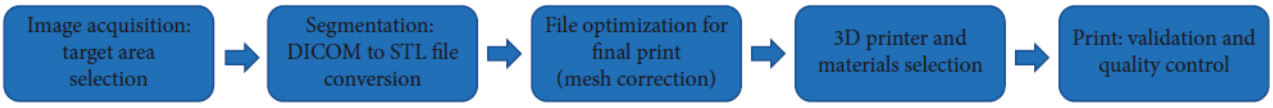

Figure 2.1: 3D Printing Workflow.

2.1 Use of customized implant for orbital cavity reconstruction

A specific workflow for the orbital floor surface reconstruction has been defined to design a custom implant. The 2D image data coming from Magnetic Resonance Imaging (MRI) and CT scan are acquired in digital imaging and communications in medicine (DICOM) format.

The DICOM data is then processed using software to create a 3D model of the anatomy depicting the defect.

The 3D model file is then imported into a design software to create the final implant design ready for additive manufacturing.

In the study of Mustafa et. Al [26] the authors present the clinical results of their method of customized reconstruction of orbital cavity defects using titanium mesh or sheet.

High resolution computed tomography (CT) data are imported and processed to create a three-dimensional (3D) image which is used to reconstruct the orbital defect. Mirror imaging of the air in the contralateral maxillary sinus is used to overcome artefact defects in the floor.

A STL model is constructed, from which titanium mesh or sheet is shaped and sized to the required contours for implantation.

Twenty-two patients were treated using this technique from 2003 to 2008.

Patients were scanned using high resolution CT with a slice thickness of 0.5 mm. The raw CT information obtained was imported in DICOM file format and processed to create a 3D image using Mimics software (Materialise NV, Leuven, Belgium).

The position of the mid sagittal plane was then established in order to be able to mirror image the sinus morphology to the defect side (Fig. 2.2).

The superior contour of the 3D sinus volume thus recreates the shape of the orbital floor.

The resulting virtual model was used to construct a stereolithographic model (Fig. 2.3) using rapid prototyping.

This model was used to enable the shaping of the titanium mesh in the laboratory to the required contours to fit the virtually repaired orbital defect.

Postoperatively, 10 patients reported early resolution their diplopia. Six patients noticed significant improvement of their symptoms with mild residual diplopia, in one direction only and at the extremes of gaze, at final review.

One patient required ocular muscle surgery. Enophthalmos resolved in eight of the nine cases. No patients developed enophthalmos or diplopia as a postoperative complication [26].

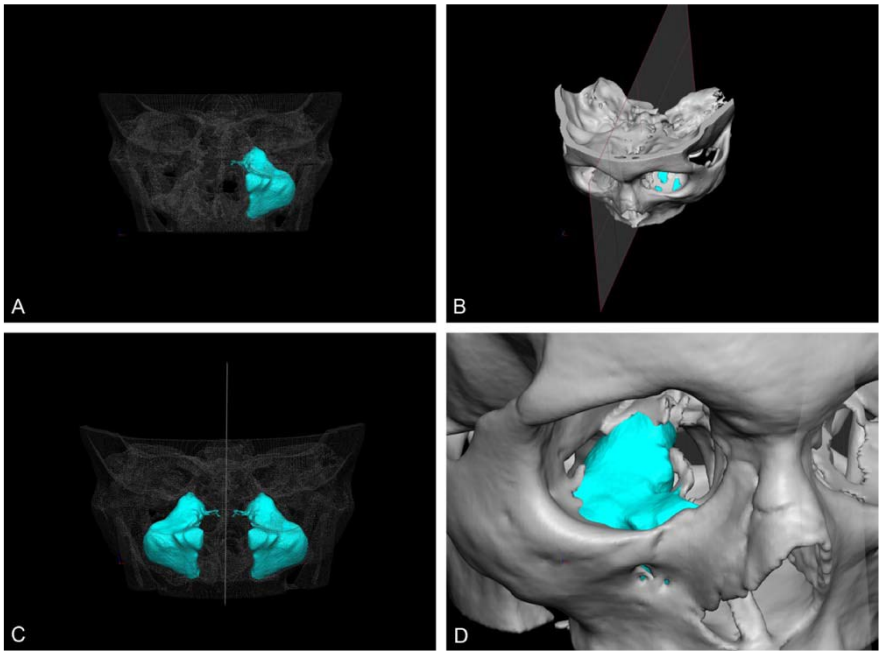

Figure 2.2: Process of virtual reconstruction of the orbital floor using the shape and position of the opposite maxillary sinus. (A) Capturing the air in the contralateral maxillary sinus. (B) Establishing a mid-sagittal plane. (C) Mirroring the maxillary sinus onto the defect side. (D) A 3D image with the virtually reconstructed orbital floor.

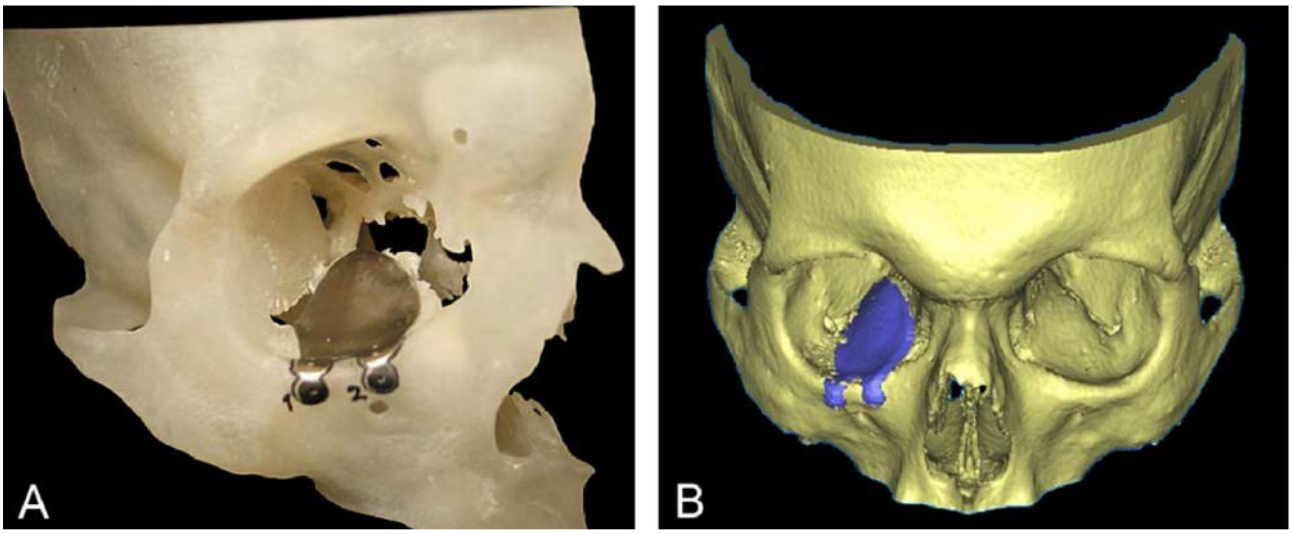

Figure 2.3: (A) Stereolithographic model with the customized titanium plate in position prior to sterilisation. (B) 3D reformatted image of a postoperative CT scan with the titanium plate highlighted.

In line with this study, Vignesh et al. [18] and Lieger et al. [27] showed the result of an orbital floor reconstruction using STL.

In the first one, aim of this case report is to highlight the precision and accuracy obtained with patient specific implants (PSI) for orbital reconstruction designed on the basis of volumetric analysis of orbital computed tomographic scan (CT) using virtual planning, computerised designing and manufacturing and stereolithographic models.

The study was performed on one patient reporting with diplopia during upward gaze and severe enophthalmos. The workflow for the 3D reconstruction was the same, a computed tomographic scan was obtained.

The data were recorded in a generic Digital Imaging and Communications in Medicine (DICOM) format and transferred to a windows-based computer workstation with computer-assisted design and computer-assisted manufacturing software.

The software converted the data for 3D reconstruction. Planning was performed by mirroring the unaffected side to the side where reconstruction was necessary.

The data of the reconstructed orbit with the determination of the planned patient specific implant were sent to the manufacturer.

The surgeon and the software designer planned the patient specific implant in titanium mesh to create its optimal shape and size [18]. Patient showed marked correction of his upward gaze diplopia and enophthalmos when a customized patient specific implant was used (Fig. 2.4).

In the 29 patients analyzed in the study of Lieger et al. [27] treated for extensive orbital fractures from January 1, 1997, through December 31, 2007 showed that the use of a CAD technique based on cross-sectional computed tomographic scans, generating an accurate stereolithographic model, enabled surgeons and technicians to plan and create the best dimension and position of the implant. Sheet titanium was then pressed to shape from a design outlined on a counterdie of the new reconstructed model.

Twenty-nine patients with late enophthalmos due to complex orbital fractures underwent successful reconstruction surgery. Two stereolithographic models, an untouched defect model and a repair model, are built using a rapid prototype machine.

To correct any irregularity, the surface of the reconstructed orbit may be smoothened with an ultrathin layer of plaster Enophthalmos was corrected in all patients (Fig. 2.5). Diplopia was improved in 14 patients, and extraocular movement was improved in 13.

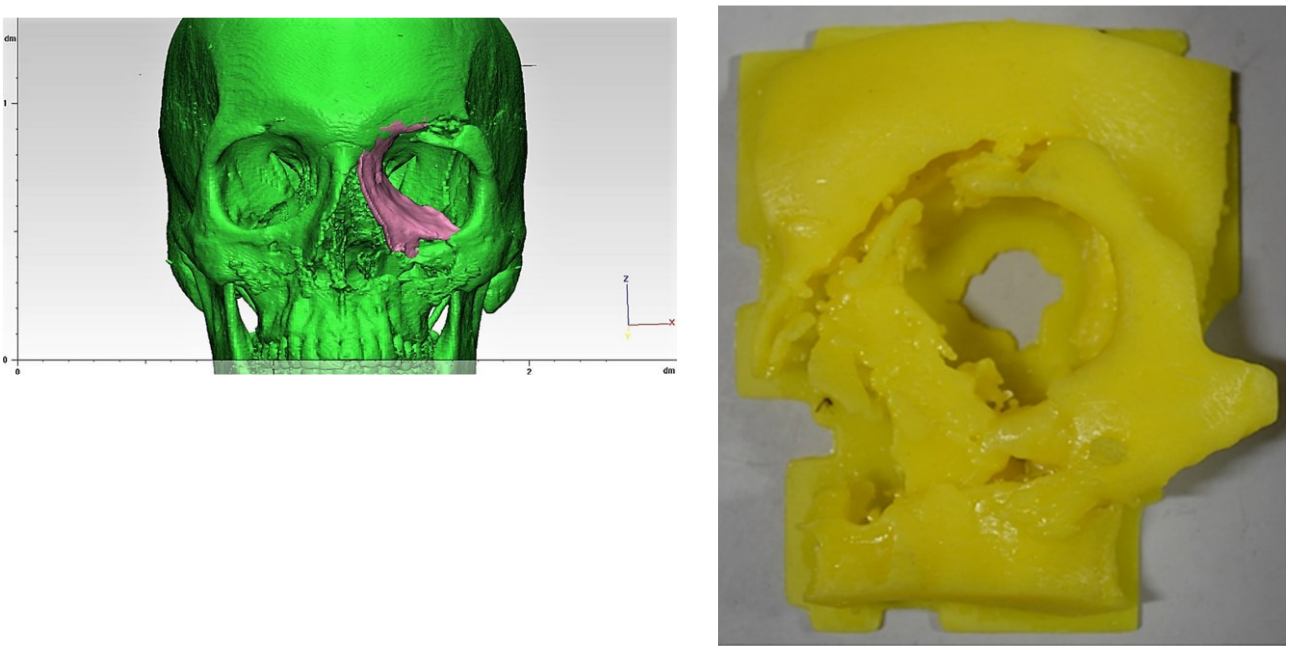

Figure 2.4: Computer Assisted Designing of implant for 3D reconstruction of fracture medial wall, orbital floor and superior orbital wall. Stereolithographic model showing fracture of orbital floor, medial wall and superior walls for treatment planning.

Figure 2.5: (A) Stereolithographic model with the customized titanium plate in position prior to sterilisation. (B) 3D reformatted image of a postoperative CT scan with the titanium plate highlighted.

2.2 Computer-assisted techniques

An innovative approach for primary and secondary reconstructions of fractured orbital cavity was through the use of computer-assisted techniques and additive manufacturing. In fact, in the study of Mandolini et al. [21].

The present case study reports on the secondary reconstruction of the skeletal orbit following untreated orbital floor fracture in a patient wearing an ocular prosthesis. The patient is a man, 64 years old, involved in a severe sport accident 35 years earlier. A specific workflow for the orbital floor surface reconstruction has been defined to design a custom implant.

First, through the 3D anatomical modelling, the geometry of the implant is shaped to fill the orbital defect and recover the facial symmetry. Subsequently, starting from the modelled implant, a customised mould is designed taking into account medical and technological requirements. After the orbital cavities reconstruction (Fig. 2.6) and the mirroring of the healthy orbital cavity on the pathological orbital cavity using Mimics (Fig. 2.7), .stl files containing the meshes of the pathological orbital cavity and of the mirrored healthy one have been imported in Rhinoceros 3D v.5.0 by McNeel Inc., a commercial 3D modelling tool, particularly used for biomedical and industrial design, which directly outputs .stl files for 3D printers and rapid prototyping systems. Thanks to its versatility, Rhinoceros 3D allowed both the reconstruction of the pathological orbital floor surface and the design of the mould by means of reverse engineering techniques [21].

Mould must satisfy several technological and clinical needs to prevent issues with the 3D printing technology and to be successfully used during surgery. The mould has been designed by using Rhinoceros (Fig. 2.8) v.5.0 in which the typical requirements were an example, sterilizable, adaptability of the mould to several prosthetic materials (titanium meshes and demineralised bone) tissue, low-cost and affordable.

The mould has been manufactured in polyamide using the Selective Laser Sintered (SLS) technique. The sterilised SLS mould has been used during orbital surgery to realise a customised orbital floor implant. In this specific case both demineralised bone tissue membrane and net-shaped titanium sheet have been modelled by the surgeon. The proposed surgical procedure solves most of the problems in terms of implant geometry, placement and cost, trauma to periorbital tissues, choice of implant material, manufacturing of custom implant, cost and surgical time. However, using the implant modelled with a custom-made mould, the surgeon does not need to re-adjust the shape and the placement of the implant, thus shortening the duration of the surgical procedure. The average duration of 1 h is reduced to approximately 35 min. This decrement in time also means a decrement in costs, as the hourly cost of an operating room is considerable [28].

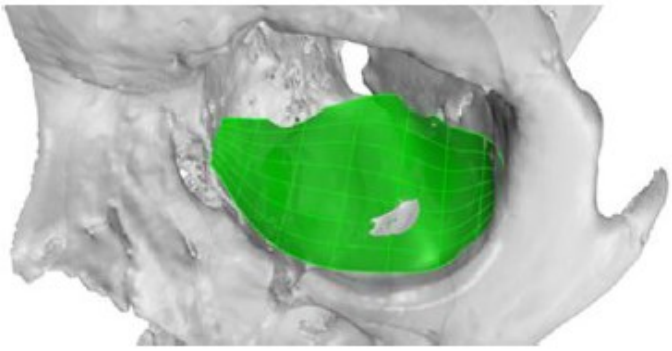

Figure 2.6: Orbital cavities reconstruction using Rhinoceros.

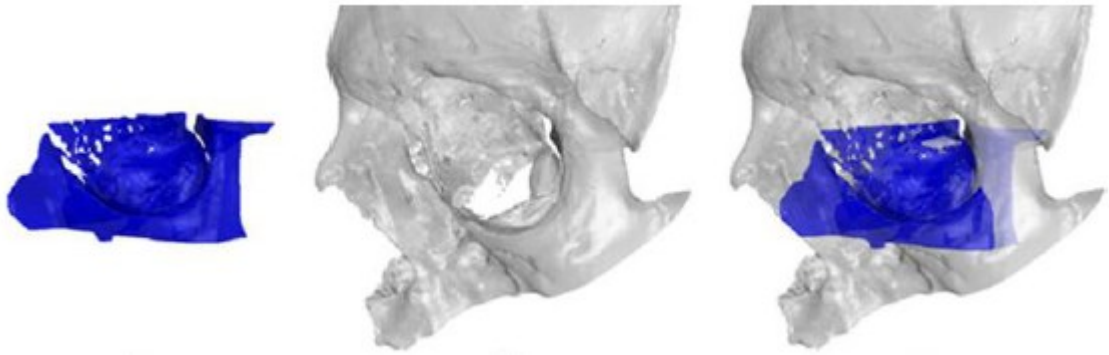

Figure 2.7: Mirroring of the healthy orbital cavity on the pathological orbital cavity using Mimics.

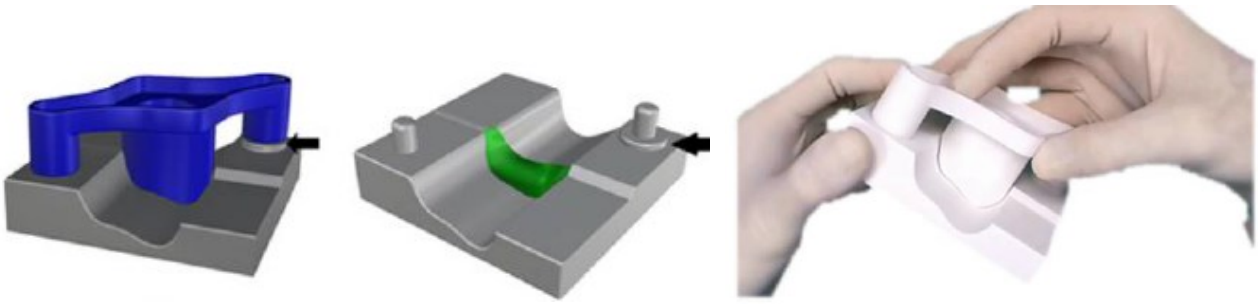

Figure 2.8: Design mould on Rhinoceros and the realization of Selective laser sintered mould during surgery.

A similar approach can be seen in the study of Kang et al. [20] in which a method for the reconstruction of the orbital floor that uses three-dimensionally (3D) printed templates to mold a customized orbital implant was analyzed. The study was conducted on 11 patients who underwent orbital cavity reconstruction using 3D-printed customized orbital implant templates. In these procedures, the orbital implant was 3D pressed during surgery and inserted into the fracture site. The workflow was more or less the same, in fact patient's orbit including the fracture site was analyzed using Mimics and 3-Matic software (Materialise, Leuven, Belgium) to create a virtual 3D orbital implant model for the fracture site, then mirror the healthy orbital cavity on the pathological one, in this way a 3D orbital implant model was then created to fit the shape and surface of the fracture site and converted into a stereolithography (STL) file. Templates and press were printed using a Projet 3510SD device (3DSystems, Inc., Rock Hill, SC) with 32 μM resolution. The implant was then placed between the upper and lower body of the templates and then inserted into a press (Fig. 2.9) [20]. Results showed that all 11 orbital cavity reconstructions (6 orbital floor and 5 medial wall fractures) were successful with no post-operative ophthalmic complications and also there was no statistically significant difference found between the tissue volume of the contralateral unaffected orbit and the affected orbit after reconstruction.

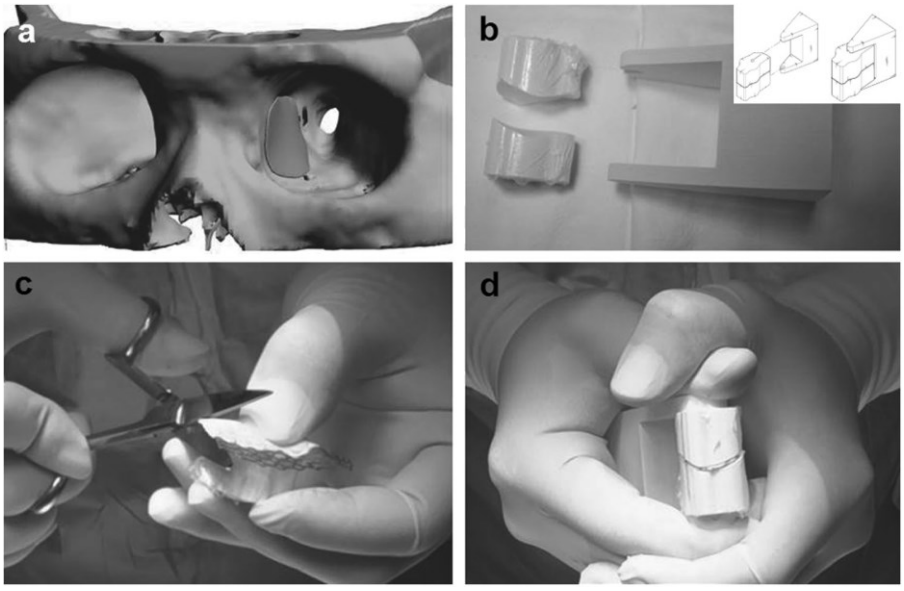

Figure 2.9: ***a-*** *Preoperative virtual 3D orbital implant model for the fracture site.* ***b-*** *Templates and press.* ***c-*** *Tracing of a template onto porous polyethylene with an embedded titanium implant and cutting out of the unnecessary parts.* ***d-*** *Insertion in the press.*

Numerous cases of reconstructive implant use have been described in the literature [29] [30]. In fact, Gander et al. [31] presented a new approach employing customized patient-specific titanium implants suitable for daily use.

These easily manufactured and implemented, ready-made patient specific implants (PSI) allow for a more cost- and time effective operating procedure. 12 Patients who underwent operations for orbital wall and/or floor fractures, between February 2014 and June 2014, were recruited.

Preoperative CT-scan data were processed using the iPlan software package (Fig. 2.10) (ver. 3.0.5, Brainlab, Feldkirchen, Germany) to generate a 3D reconstruction of the affected orbit, using the mirrored non-affected orbit as a template.

Then, transfer of the 3D coordinates of the implant, from iPlan 3.0.5 to the manufacturing software (KLS Martin), circumferential implant cushions should be created, although laser-sintered, individually manufactured implants exhibit greater stiffness compared with manually adjusted titanium meshes and at the end positioned (Fig. 2.11).

All patients underwent reconstruction of the orbital wall or orbital floor via PSI showed visual impairments, no reposition of the implant post-surgery, time between 30 to 36 min during surgery and days for manufacturing 4 days.

In most of the studies, Autografts, allograft, and alloplastic materials are used to reconstruct the orbital floor, but there is no consensus on which material is the best [32]. A key role in the reconstruction of the orbital floor was the use of titanium.

Titanium has excellent biocompatibility and demonstrates integration in adjacent bone, which results in low infection rate and rare postoperative migration of implants after titanium reconstruction.

Al-Anezi et al. [33] showed the results of the use of a titanium mesh for the reconstruction of the orbital cavity in cases of orbital blowout fractures. From January 2014 to December 2016, 24 patients with orbital blowout fractures managed surgically using titanium mesh were evaluated. The workflow was more or less similar to the other studies. 15 of 24 were males and 9 were females.

11 of 12 patients with diplopia improved and one patient had persistent diplopia.

All patients with enophthalmos or ocular motility disorders improved, only one patient developed late enophthalmos and treated using iliac bone graft.

There were no intraoperative complications such as damage to the globe or the optic nerve or unexpected hemorrhage.

There were no postoperative complications like bleeding, vision loss, infection, and implant extrusion, or malposition, orbital congestion, epiphora.

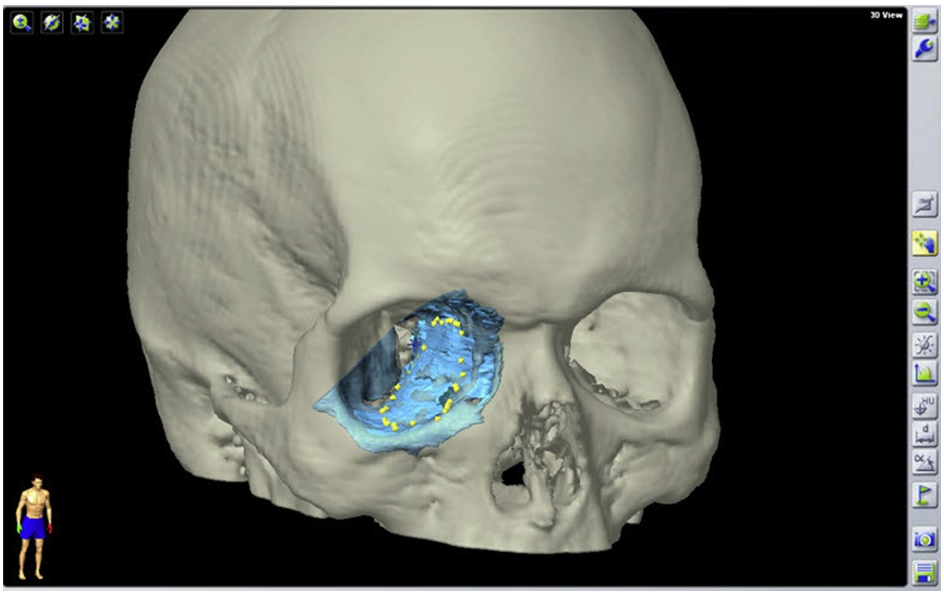

Figure 2.10: Determination of the prospective implant's extent using iPlan.

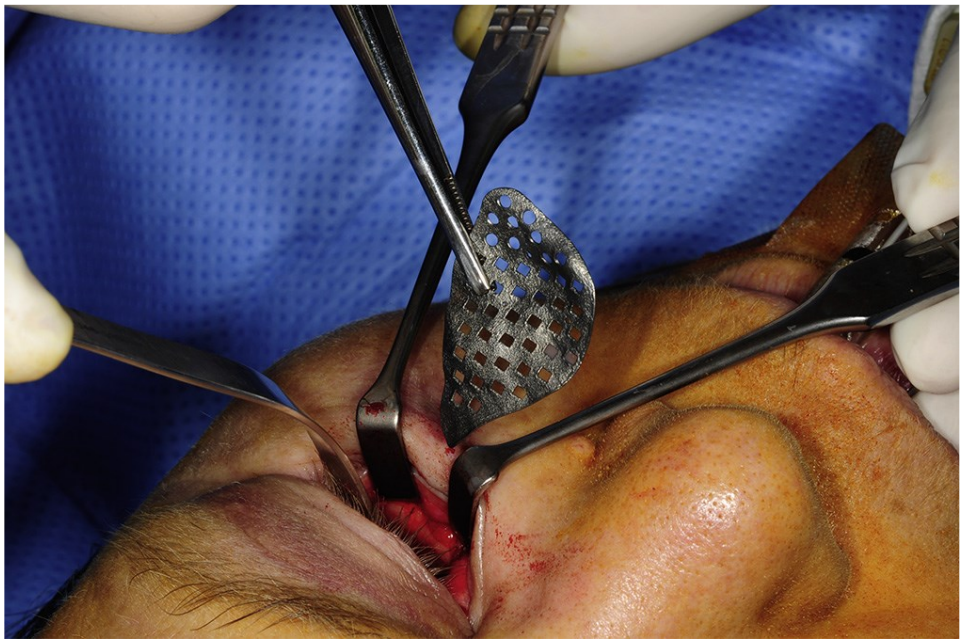

Figure 2.11: Transconjunctival, post-septal PSI placement.

In the treatment of enophthalmos and persisting diplopia due to orbital cavity fractures, 3D orbital reconstruction remains the primary goal.

It is generally agreed that the main reason for enophthalmos is an increase in volume of the posterior segment of the orbit and changes in the deep orbital cone area [34].

The use of rapid prototyping and stereolithographic models has proven benefits in orbital reconstruction [35]. In 1999, Hoffman et al. [36] reported the use of stereolithographic models for the planning and fabrication of copy-milled customized ceramic implants for orbital cavity reconstruction in a series of six cases with promising postoperative outcomes.

The decision whether to treat surgically or not, the choice of surgical approach for access and of material for wall defect reconstruction have all been hotly debated.

Sugar et al. [37] described the original use of titanium mesh implants for the reconstruction of moderate size orbital cavity defects where it was found to be a valuable material with minimal complications.

In a study of Ellis & Tan et al [19] demonstrated that although both bone grafts and titanium mesh could be successfully used in orbital cavity fracture repair, titanium was shown to provide better and more accurate anatomical reconstructions than those done with autogenous calvarial bone grafting. In these studies, the production cost of these customized titanium implants was currently less than commercially available titanium mesh sheets or preformed implants from all leading manufacturers. the use of titanium mesh for orbital cavity reconstruction has been shown to be safe and effective. Custom made titanium implants are easy to manipulate, insert and anchor.

They accurately reproduce orbital contours thus restoring orbital volume. This leads to reduced operative time and an improvement in functional and aesthetic outcomes of post-traumatic orbital reconstruction.

In line with the previous study, Mohamed et al. [38] instead, compared the use of prefabricated titanium implants versus custom-made computerized assisted plate in the reconstruction of the internal orbital defects but there was a non-significant difference between the studied groups in the degree of accuracy of volume correction and in the correlated correction of corneal projection despite of the great degree of preoperative orbital volume distortion in both groups.

There was no statistically significant difference between both groups, in the accuracy of correction of the degree of hypoglobus, palpebral fissure width narrowing, reduction of visual acuity, diplopia and motility restriction [39].

2.3 Clinical studies and results

The use of preformed implants for orbital floor and medial wall reconstruction saves time and renders traumatic intraoperative bending and adjustment of the implants unneeded, which is of particular importance in cases of poly trauma.

However, non-statistically significant differences were found between it and the custom individually computer assisted implants (Table I).

The realization of a mould for the orbital reconstruction instead allow some advantages, in fact, in the study of Mandolini et al. [21] decrease the surgical time and patient morbidity, decrease the surgery cost and was a fast preoperative planning procedure, also in the study of Kang et al. [20] it was used porous polyethylene with embedded titanium implants because it has the advantageous properties of both porous polyethylene and titanium. Titanium mesh has significant tensile strength and can be easily contoured to fit the shape and surface of the fracture site because of its malleability and memory [40], which are essential properties for 3D molding. In conclusion, the use of the right material or the procedure to be performed to restore the fractured orbit remains a heated debate today.

Author	Title	Aim	Types of implants	Positioning of implant	Advantages	Disadvantages
Mustafa et al. [26]	Customized titanium reconstruction of post-traumatic orbital wall defects: A review of 22 cases	-CT data are imported and processed to create a 3D image. -Mirror process. Stereolithographic model.	-Titanium mesh	/	-Safe and effective -Customized titanium implants accurately reproduce orbital contours.	-3 patient present problem after surgery.
Vignesh et al. [18]	Three-dimensional reconstruction of late post traumatic orbital wall defects by customized implants using CAD-CAM, 3D stereolithographic models: A case report	-3D CT data -Mirror process -Customized implant	-Titanium mesh	-The surgeon and the software designer planned the patient specific implant in titanium mesh to create its optimal shape and size. -Flanges were added to the design to ensure perfect sagittal positioning and screw holes were also designed for fixation along the orbital rims.	-Correction of diplopia and enophthalmos	/
Lieger et al. [27]	Computer-assisted design and manufacture of implants in the late reconstruction of	-CT data -Mirror process. Stereolithographic model is constructed	-Titanium mesh -Autogenous bone -Hydroxyapatite	-All patients received perioperative prophylactic antibiotic therapy. -Surgery was performed with the	-Improve diploplia and eye movements.	/

	extensive orbital fractures			patient under general anesthesia. -Subciliary or lower eyelid/midtarsal incisions were used to expose the infraorbital rim and the orbital floor. -Subperiosteal dissection was used to identify stable bony structures around the defect. -The sterilized implant was inserted and screwed to the bone using the predrilled holes.		
Mandolini et al. [21]	Selective laser sintered mould for orbital cavity reconstruction	-3D CT data -Mirror process -Customized implant	-Titanium mesh	-The mould has a reference system that allow the surgeon to understand how orient the implant in the eye socket.	-Low cost -Reduce time -Good placement	/
Kang et al. [20]	Generation of customized orbital implant templates using 3-dimensional printing for orbital wall reconstruction	-CT data -(3D) printed templates -The orbital implant	-Titanium mesh	-Orbital floor fractures were exposed through a preseptal transconjunctival incision and medial orbital wall fractures through a transcaruncular incision. -Orbital wall defects were reconstructed using a customized orbital implant. -The implant was then placed between the upper and lower body of the templates and then inserted into a press.	-No ophthalmic complications -Improve eye movements	-High cost -Persisting diplopia in one patient
Gander et al. [31]	Patient specific implants (PSI) in reconstruction of orbital floor and wall fractures	-CT data, processed throught iPlan to reconstruct 3D image, -Mirror process -Implant design -Intraoperative navigation	-Titanium mesh	-PSI allow to see the correct positioning of the implant thanks intraoperative navigation.	-PSI allows precise reconstruction of orbital fractures	-High cost -Require time

Al-anezi et al. [33]	Role of Titanium Mesh as a Reconstruction Material for Orbital Floor Defects in Cases of Orbital Blowout Trauma	-CT data -Mimics -Mirroring of healthy orbital cavity -Reconstruction of pathological orbital cavity	-Titanium mesh	/	-Improved diplopia	-One patient had persisting diploplia
Hoffman et al. [36]	Orbital reconstruction with individually copy-milled ceramic implants	-CT data are imported and processed to create a 3D image. -Mirror process. Stereolithographic model is constructed	-A titanium/porous polyethylene implant	-A titanium/porous polyethylene implant was cut manually. -The implant was contoured intraoperatively. -The molded implant was then applied to the reconstructed orbital model.	-Low cost -Reduce time -High accuracy	/
Sugar et al. [37]	Titanium mesh in orbital wall reconstruction	-Use of titanium mesh implants for the reconstruction of moderate size orbital wall defects	-Titanium mesh implants	/	-Good results with the use of titanium -Improve diplopia	/
Ellis et al. [19]	Assessment of internal orbital reconstructions for pure blowout fractures: Cranial bone grafts versus titanium mesh	-Use of bone graft and titanium mesh for repairing orbital wall	- Bone graft and titanium mesh	/	-Correction of diplopia and enophthalmos	-High cost of titanium
Mohamed et al. [38]	Orbital Defect Reconstruction: the Use of Preformed Titanium Plates Versus Custom-Made Titanium Computer Assisted Implants	-Use of prefabricated titanium implants versus custom-made computerized assisted plate in the reconstruction of the internal orbital defects	- Preformed Titanium Plates; - Custom-Made Titanium Computer Assisted Implants	/	-No ophthalmic complications -Reduce time	-High cost of prefabricated titanium implants

Table I: Different approaches for the reconstruction of the orbital floor.

3- DESIGN OF MEDICAL DEVICES FOR IMPLANT SHAPING AND POSITIONING

Patients who suffered disruption of the eyeball following direct or indirect ocular trauma often present an untreated fracture of one or more orbital cavities. In particular:

- Fracture of the floor and/or the medial wall of the orbit;
- Asymmetric ocular prosthesis;
- Critical ocular and orbital volume.

The ocular prosthesis is critical for adequate volumetric repair, and one of the main problems associated with designing well-fitting orbital prostheses is obtaining an accurate midfacial plane to restore the facial symmetry [21]. The primary goal for orbital reconstruction is to repair the fractured cavity by restoring skeletal cavity, orbital volume, function and aesthetics. The application of 3D printing in medicine can provide many benefits. The current work focuses on the development of a procedure to design a customized medical implant and a device capable to guide the surgeon in the insertion of a titanium mesh prosthesis in the orbital cavity. To date, surgeons have three main choices for the reconstruction of orbital cavities, but some drawbacks are evident in each of them [21]. The first one consists in shaping the implant directly on the patient orbital cavity during the surgery but cannot guarantee an accurate definition of implant geometry and positioning, resulting in long surgical time and trauma for periorbital tissues caused by the unavoidable repetitive trial fitting of the implant. The second one consists in implanting a preformed titanium plate or a 3D printed custom-made titanium mesh but the main issue of the second and third techniques is related to the high cost of implants manufacturing processes. Indeed preformed titanium orbital meshes or plates cost between €250 (KLS Martin, Tuttlingen, Germany) and €600-800 (Synthes, West Chester, PA), while electron beam melted or direct metal laser sintered orbital implants cost between €3,000 and 5,000 [41]. The last one consists in modelling the implant on the 3D printed mould of the pathological orbital cavity, but the main problem of the third technique is related to time. In fact, the surgeon needs to first manually model the implant on the mould surface, and then he/she must re-adjust the implant placement and geometry on the patient's orbital cavity [41]. In this study, a titanium mesh prosthesis was chosen because it has high biocompability, is malleable, is easily adaptable to the shape of the orbital defect and is not osteoinductive and resorbable. The aim is to find an innovative method, for the orbital wall's reconstruction, to:

- Define the geometry of the implant;
- Define the placement of the implant;

- Leave the choice of the implant material to the surgeon during surgery; A computer-assisted approach, based on anatomical modelling, custom-made mould fabrication and design of a device for the insertion of the prosthesis in the fractured cavity via selective laser sintering (SLS) is proposed
- Be low cost.

The proposed method is based on seven points procedure:

1. Anatomical modelling of orbital cavity surface (Computer-assisted approach);
2. Design of custom-made mould (Computer-assisted approach);
3. Design of a medical device to help the surgeon in the insertion of a titanium mesh prosthesis (Computer-assisted approach);
4. Fabrication of customised mould (Selective laser sintering);
5. Fabrication of a medical device (Selective laser sintering);
6. Shaping of orbital implant (Immediate and in office);
7. Insertion of prosthesis (Immediate and in office).

3.1 Orbital cavity modelling

A specific workflow for the orbital cavity surface reconstruction has been defined to design a custom implant. The acquisition of the patient's CT images is necessary for 3D virtual reconstruction of the skull (Step 1), first, the bony areas have been extracted from each slice, and then, the 3D visual models have been obtained by stacking the segmented slices (Step 2). Then, the healthy orbital cavity has been mirrored on the pathological one (Step 3) (Fig. 3.1).

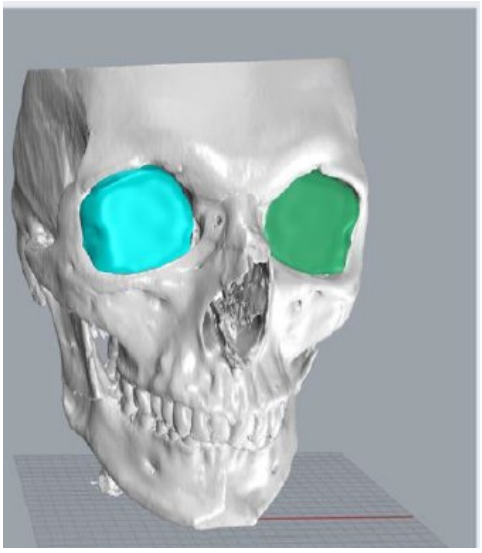

Figure 3.1: Mirror of the fractured cavity (blue) on the healthy one (green).

Thus, the .stl files containing the meshes of the pathological orbital cavity and of the mirrored healthy one have been imported in Rhinoceros 3D v.6.29 byMcNeel Inc., a commercial 3D modelling tool, particularly used for biomedical and industrial design, which directly outputs .stl files for 3D printers and rapid prototyping systems.

Thus, the mirrored healthy orbital cavity has been adjusted and fitted on the pathological one to reconstruct the pathological floor surface (Step 4).

Then, definition of spline curves on the mirrored healthy orbital floor for the reconstruction of the pathological orbital floor through Rhinoceros (Step 5).

The last steps consist in reconstruction of the pathological cavity surface (Step 6), morphing and adjustment of the reconstructed orbital surface on the fracture using Rhinoceros (Step 7) (Fig. 3.2).

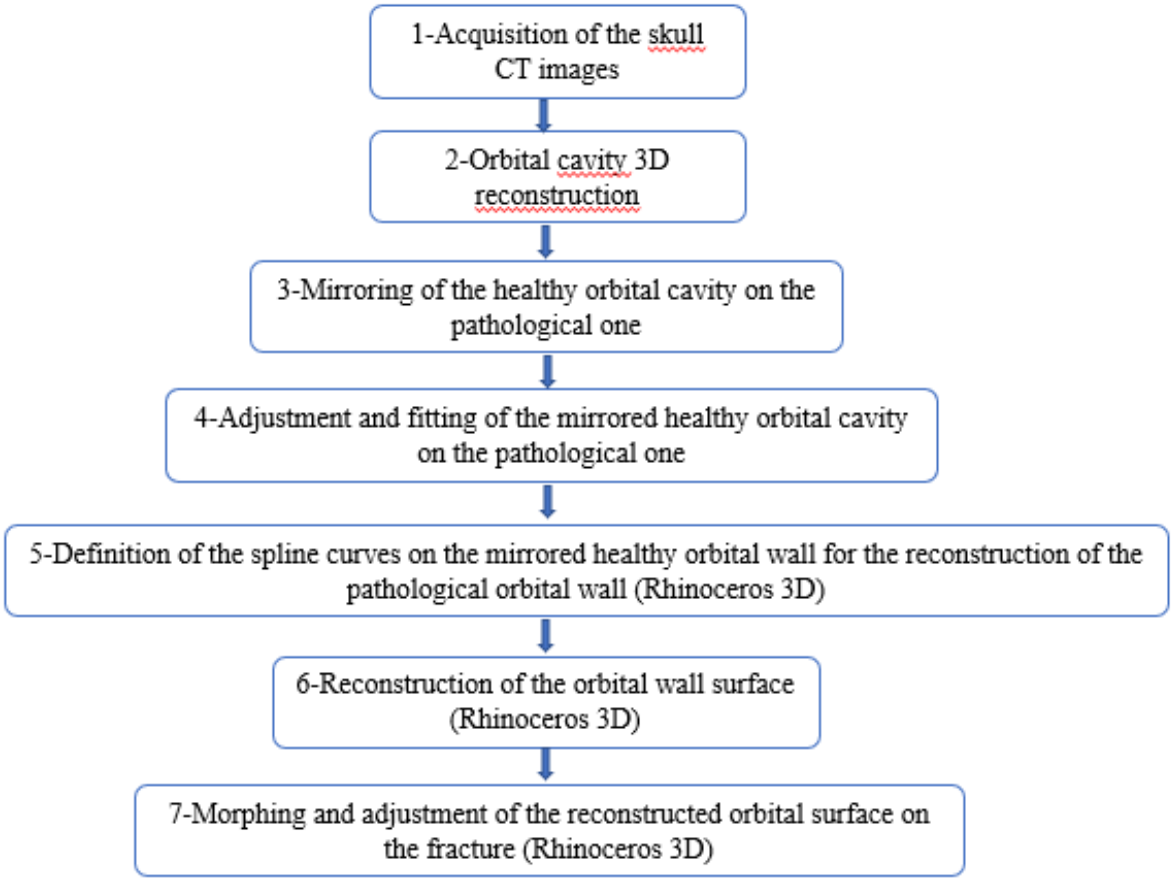

Figure 3.2: Workflow of 3D virtual reconstruction of orbital floor.

3.2 Mould requirements, design and manufacturing

The mould must satisfy several technological and clinical needs to prevent issues with the 3D printing technology and to be successfully used during surgery. For this reason, two tables of requirements about the mould have been defined (Table II, Table III).

The mould has been designed used Rhinoceros v. 6.29 to satisfy the medical and mechanical requirements. The mould is designed starting from the reconstructed orbital cavity surface. In fact, present:

- Absence of undercuts;
- The square base of the die ensures a large contact area;
- The hollow shape of the punch: Reduces the material consumption, improves the handling, allows the side areas of the implant to deform freely, reducing the needed force.
- Two lateral guides (pins with relative holes) guarantee the correct alignment between die and punch;
- The referencing system allows the surgeon to easily understand how to orient the implant.

In this case study, the mould has been manufactured in polyamide using the Selective Laser Sintering technique. SLS has been selected for the following advantages:

- Possibility to manufacture autoclave sterilizable parts;
- Small series produced in one manufacturing process;
- Fast and economical process;
- Functional;
- High accuracy;
- Durable and versatility of material;

SLS process is fast and economical and no support is needed during the manufacturing process. Moreover, SLS-manufactured objects are autoclave sterilisable [42] [21].

AIM	**CLINICAL REQUIREMENTS**
1.To introduce the mould in the operating room	The mould must be sterilisable
2.To choose the implant material during surgery	Adaptability of the mould to several prosthetic materials (Titanium meshes)
3.Economic benefit to the patient	The mould must be low-cost and affordable
4.To understand easily the cutting perimeter	The mould must model the implant and suggest the cutting area
5. To orient unequivocally and easily the implant during the surgery	The mould must present a reference system to indicate the orientation of the implant to the surgeon

Table II: Clinical requirements for the design and manufacturing of the mould.

AIM	MECHANICAL REQUIREMENTS
1.The structural strength of the mould must be guaranteed	A design limit strain and a safety factor have to be defined on the basis of the mould material
2. Easy opening and closing of the mould	The coupling tolerances on the different parts of the mould must be suitable for the additive manufacturing process
3. Minimization of the manufacturing costs	The overall dimensions of the mould must be minimum

Table III: Mechanical requirements for the design and manufacturing of the mould.

3.3 Medical device requirements, design and manufacturing

The medical device must satisfy several technological and clinical needs to prevent issues with the 3D printing technology and to be successfully used during surgery.

3.3.1 Medical device requirements

For the realization of the medical device, it was important to define some parameters that are fundamental for the design:

1. Requirements;
2. Functions;
3. Specification;
4. House of quality;

Requirements are the designers detailed breakdown of what the product should do and achieve without providing solutions. In fact, for the design of the device, the requirements that best meet the purpose of the study have been defined. The goal is to design a medical device that is a valid alternative to the classic instruments used for inserting a prosthesis in the fractured orbit. In this regard, the device must be able to attach itself to a biocompatible material. As mentioned in the previous sections, materials such as titanium mesh or demineralized bone plate are the most used to restore the orbital cavity. Therefore, an important requirement is the ability of the device to attach itself to a biocompatible material for its use during the operation. In line with this requirement, the device must be used to treat fractures of the orbital cavity, therefore suitable for orbital floors and walls. In fact, unlike the classic instruments on the market, which are used for any type of implant, the device must be able to grasp deformed prostheses, such as titanium mesh or demineralized bone plate.

In order to use the device in the operating room, the device must be sterilizable. Sterilization can be achieved by various means, including heat, chemicals, irradiation, high pressure, and filtration. After sterilization, an object is referred to as sterile or aseptic. For this reason, the choice of making a device whose material is sterilizable was another important requirement to be met.

The aim of this study is to design and manufacture a low-cost, high-performance and reliable non-invasive device. Currently, in various sectors of medicine such as the facial and maxillofacial surgery sector, there is a growing need for innovation, especially as regards the tools available to perform corrective treatments. Therefore, it was decided to design an economical device that is a valid alternative to the instruments on the market suitable for these types of operations. Two other important requirements for the design of the device are its safety during use and its use. In fact, medical products can be defined based on their intended use either for use on a single person (single use) or with multiple people over time (reusable). For reusable items, it is important that these can be used safely on each patient for the designed life of the device. Such devices can range from high-risk surgical devices that contact "sterile" areas of the body, including blood, to devices that can only touch the skin of healthcare professionals or their patients.

Safety aspects include the reduction or removal of disease-causing microorganisms (due to the risk of infection), toxicity, electrical or mechanical failures, and other adverse patient or staff events that may occur while using a damaged device or malfunctioning. For this reason, a device requirements table has been defined (Table IV).

AIM	**REQUIREMENTS**
1.To choose the correct material	Biocompatible material
2.Economic benefit to the patient	Low cost
3.To introduce the device in the operating room	Device must be Sterilizable
4.To use the device several times	Reusable
5.To be secure	Ergonomic
6. To orient unequivocally and easily the device during the surgery	Easy to use
7.To choose the implant material during surgery	Usable for deformation prostheses
8. To treat orbital fractures	Suitable for orbital floors and walls

Table IV: Requirements for the design and manufacturing of the device

Once a list of requirements has been established, the next two steps are to prioritize and organize these requirements so that the designer is aware of the essential requirements as well as the ones that can be compromised due to conflict, cost or other reasons. Requirements need to be discussed in terms of what has to be done and not how it is to be done. It is important that the requirements specification not restrict the design space unnecessarily or bring in assumptions about how a system will be designed too early.

The next step consists of the definition of functions. Functions are solution neutral engineering actions that the product will perform. Functions should consider 'what' the product does (the problem) and not 'how' it does it (solution). The overall function of a product is the relationship between its inputs and output. The function of the product can be further broken down to sub functions that identify purposive actions that the product is meant to perform. Functions play an important role in device design. The device, to be used to restore the fractured orbital floor, must be able to provide feedback to the surgeon for the correct positioning and orientation of the custom-made implant. The low-cost tools used to treat these types of operations do not provide correct feedback for orienting and positioning the implant. For this reason, a prototype has been proposed that reflects these two functions.

Furthermore, the gripping mechanism of the implant is different from classic instruments. In fact, it uses a mechanical type grip mechanism while the low-cost tools present use a gripper mechanism. Based on this information, the functions suitable for the device are as follows:

1. Position the prosthesis correctly;
2. Correctly orient the prosthesis;
3. Give feedback on correct positioning;
4. Give feedback of the correct orientation;
5. Hook the prosthesis;
6. Disengage the prosthesis.

Specifications is the last step in defining the problem before you begin to suggest possible solutions. The product specifications are the first step in the process of transforming product ideas into approved product development effort. In fact, a product requirements document (PRD) is a document containing all the requirements to a certain product. It is written to allow people to understand what a product should do. Quality Function Deployment, or QFD, is a method used to identify critical customer requirements and to create a specific link between customer requirement and design specifications. Then, typical specifications for the realization of a device are (Table V):

Category	Specification	Unit of measure	Minimum value	Maximum value	Value
Geometry	Dimension control / dimensional tolerance	mm	0	0.5	-
Materials	Resistant to electromagnetic disturbances	-	-	-	Yes
User signal	Correct positioning / orientation feedback	-	-	-	Acoustic / Visual
Security	Uncertainty / accuracy of positioning / orientation	mm	-	-	0.5
	Need to recalibrate the device	-	-	-	No
Production	Productive process	-	-	-	3D printing Sintering
	Assembly by means of quick couplings	-	-	-	Yes
Economy	Cost	-	0	100	-

Table V: Specifications for the realization of a device.

The organising framework for the QFD process is a planning tool called the "house of quality" (Table VI).

This is the last step and is a method that allows each stage of the design process to be measured quantitatively on how well it is achieving the previous stage and, hence, how good the design is.

A house of quality chart is drawn to measure specifications against initial requirements.

This cascading method allows a follow through of the entire design process to measure how each stage of the design process addresses the initial requirements set by the customers.

The prioritized requirements are listed as rows along with their importance ratings (1 to 9, 9 being the most important). Specifications are listed as columns.

Each specification is then rated as a correlation to each requirement.

This is to find out how well each specification addresses each requirement. If there is no correlation, the grid space is left blank. If there is a slight or weak correlation, rate as 1.

If there is medium correlation, rate as 3. If there is high/strong correlation, rate as 9.

The absolute importance ratings of the specifications as measured against the prioritized requirements.

This is achieved by multiplying each specification rating by its corresponding requirement importance rating and adding up the respective columns to get the absolute importance rating for that specification.

The relative importance ratings and these values are the absolute importance ratings weighted relative to each other.

Here, the highest absolute rating becomes the benchmark value and is given a relative importance of 9.

All other specifications are then compared to this value.

Then, in the last two columns, the benchmark value of each requirement is measured against competing products in the market.

The objective here is to determine how the customer perceives the competition's ability to meet each of the requirements.

Usually, customers make judgments about the product in terms of comparison with other products. This step is very important because it shows opportunities for product improvement.

An accurate analysis of this table shows that a high correlation between requirements and specifications was between the ease of use of the device and providing correct positioning and orientation to the device.

For this reason, the device must be designed in such a way as to be able to help the surgeon insert the prosthesis in a completely simple and effective way.

Furthermore, it is possible to verify another high correlation between the choice of materials used for the reconstruction of the orbital cavity and the production.

Therefore, to fully satisfy this correlation it is important to create a device capable to attach itself to a biocompatible material.

The low cost and reuse requirements are perfectly suited to the production specification because the aim is to design a device that can be made several times reducing development costs and be able to be reused several times ensuring safety during its use in the operating room.

In conclusion, as a relative weight, the percentages of production and economy are high, referred to specifications.

So, the device must be low-cost, reusable, must be used to restore orbital cavities, and must be able to use deformed prostheses.

Slightly lower is the percentage of the specification of accuracy / uncertainty in positioning the prosthesis correctly but to be taken into consideration as the device must be able to provide the surgeon with correct feedback on the correct positioning and orientation of the prosthesis.

			Customer Competitive Assessment							
Relative Weight	**Customer Importance**	**Customer Requirements**	**Geometry**	**Economy**	**Feedback good positioning/orientation**	**Uncertainty/Accuracy posiztioning/orientation**	**Production**	**Necessity to calibrate the device**	**Our Product**	**Competitor 1**
8%	10	**Biocompatible Material**	▽	●	▽	●	○	▽	5	5
8%	10	**Sterilizable**	○	●	▽	●	●	▽	5	5
6%	8	**Reusable**	○	●	▽	▽	●	○	5	5
6%	8	**Low cost**	●	●	○	○	●	●	4	2
7%	9	**Preferible Material: Titanium mesh, Demineralized bone plate**	▽	○	▽	○	●	▽	5	5
7%	9	**Suitable for orbital floors and walls**	●	○	○	○	○	○	5	5
5%	6	**Ergonomic**	●	○	▽	▽	○	▽	3	5
7%	9	**Easy to use**	○	▽	●	○	○	●	5	5
8%	10	**Usable in the operating room**	○	○	▽	○	○	○	5	5
		Importance Rating Sum (Importance x Relationship)	379.39	490.84	319.85	417.56	480.15	327.48		
		Relative Weight	12%	15%	10%	13%	15%	10%		

RELATIONSHIP	WEIGHT
Strong	9 ●
Medium	3 ○
Weak	1 ▽

Table VI: House of quality.

3.3.2 Design and manufacturing of medical device

The device also has been designed used Rhinoceros v. 6.29 to satisfy some characteristics. Fixation of the implant to the instrument was provided by a grip mechanism. The coupling between the instrument and the implant was designed in such a way that the connection could withstand pressure forces. The connection between the instrument and implant is unique and since no part of the instrument interferes with the region inferior to the screw holes, the implant can be fixed to the infraorbital rim without removing the instrument first. After the implant is fixed, the instrument can be unhooked from the implant. The SLS was also used for the medical device.

4-CASE STUDY

The 2D image data coming from MRI and CT scan are acquired in digital imaging and communications in medicine (DICOM) format. The DICOM data is then processed using software as MIMICS (Materialise, Belgium), to create a 3D model of the anatomy depicting the defect. The 3D model file is then imported into a design software Rhinoceros v.6.29 (Fig. 4.1) to create the final implant design ready for additive manufacturing. The conversion of the 3D files to STL format, performed by biomedical software, generates a mesh of triangles, so that it can adequately represent the complex topography of the craniomaxillofacial region [43]. For the realization of the prosthesis, the relative mould and then, the medical device, the fracture of the orbital floor was simulated. For treatment it has been decided to create a digitally designed and Additive Manufacturing patient-specific alloplastic implant to achieve anatomically correct shape of the orbital cavity.

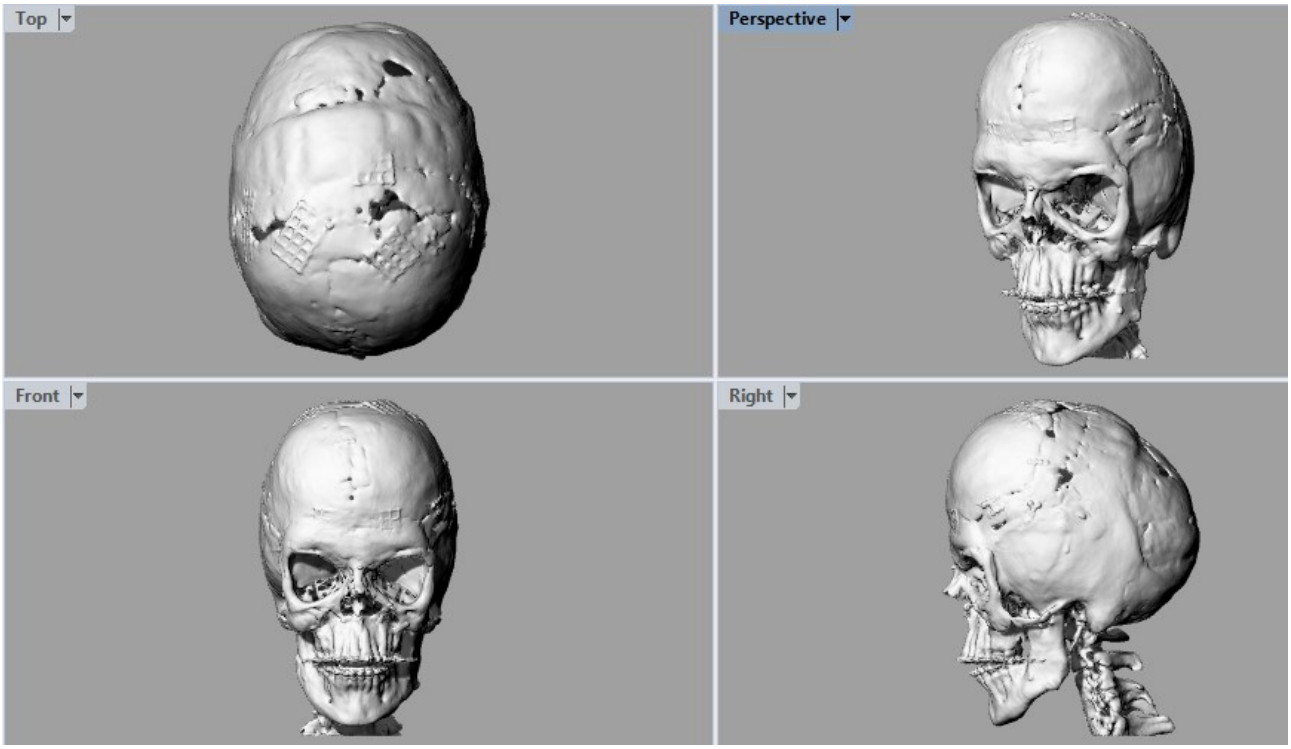

Figure 4.1: The computed tomography (CT) image of the case study is shown in Rhinoceros v.6.29 software.

4.1 Modelling the implant

Traditionally, implants have been manually bent and shaped, either preoperatively or intraoperatively, with the help of anatomic solid models, but designing implant with Rhinoceros software obviates the manual procedure and may result in more accurate and cost-effective implants. The geometry of the orbital implant can be created by mirroring the shape of the facial structure from the opposite side and repositioning it on the actual side. In this case study, the fracture of the orbital floor of the left eye was simulated. Flowchart for virtual parametric reconstruction of orbital floor is as follows:

1. Start from the acquired 3D image of the case study;
2. Cut plane;
3. Intersection between the created planes and the skull;
4. Definition of the curves of the implant;
5. Creation of the prosthesis.

So, all the procedure has been developed using the commercial 3-D modelling software Rhinoceros version 6.29, developed by Robert Mc Neel & Associates. It focuses mainly on non-uniform rational B-splines (NURBS) mathematical model that allows to accurately represent curves, surfaces, solids, free form shapes.

Creating an editable non-uniform rational B-splines NURBS surface from complex scan data can be a challenging proposition, especially when the original scanned surface is irregular and not smooth in the conventional sense.

In the following focus on workflow that allows an editable surface to be produced whilst maintaining the irregular qualities of the target surface the workflow as described attempts to find a balance between the irregular target and the well-structured Rhino surface.

The first step for the realization of the custom-made implant consists in creating vertical and parallel planes. These planes were used to cut the white mesh in order to obtain curves (Fig. 4.2). First of all, for the creation of the planes, the procedure was to open a new Rhino file and choose Big Objects Millimetres from the template options. Import the STL data into Rhino and navigate to your STL file. Then, push on the lateral “Sidebar”, in which there are all functions, and press on “Rectangle”. After the creation of a rectangle, select on the lateral sidebar the command “Rectangular series”, in particular the small triangle, and press the button “Linear series”. In this way, it was possible to create a series of ten vertical plane. To complete this step, in tabbed toolbar, select the section “mesh tools” and press on the command “Mesh from surfaces / polysurfaces” to create a series of rectangular meshes.

Through the command “Mesh intersect” it was possible to obtain a series of polylines curves generated by the intersection between the vertical planes and the mesh (Fig. 4.3).

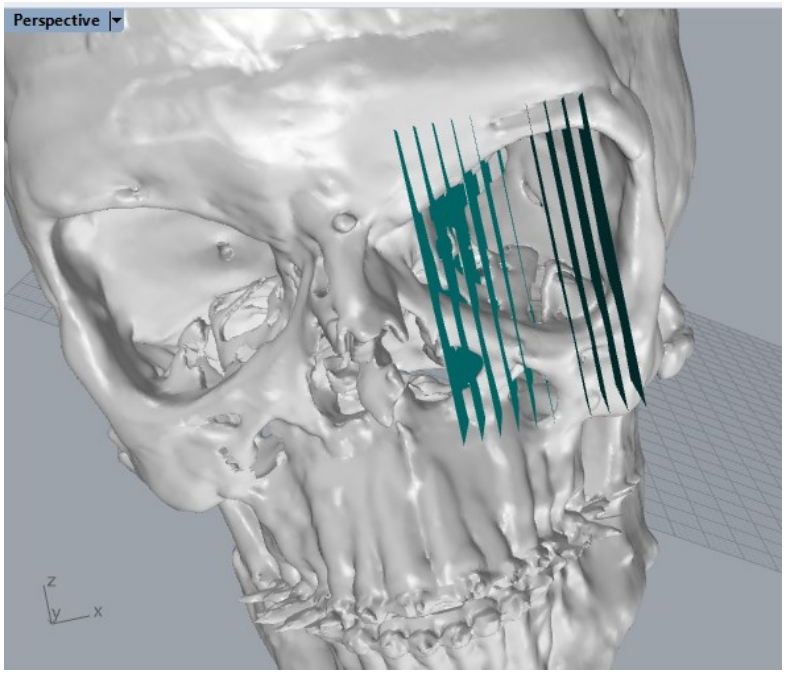

Figure 4.2: Creation of vertical and parallel planes.

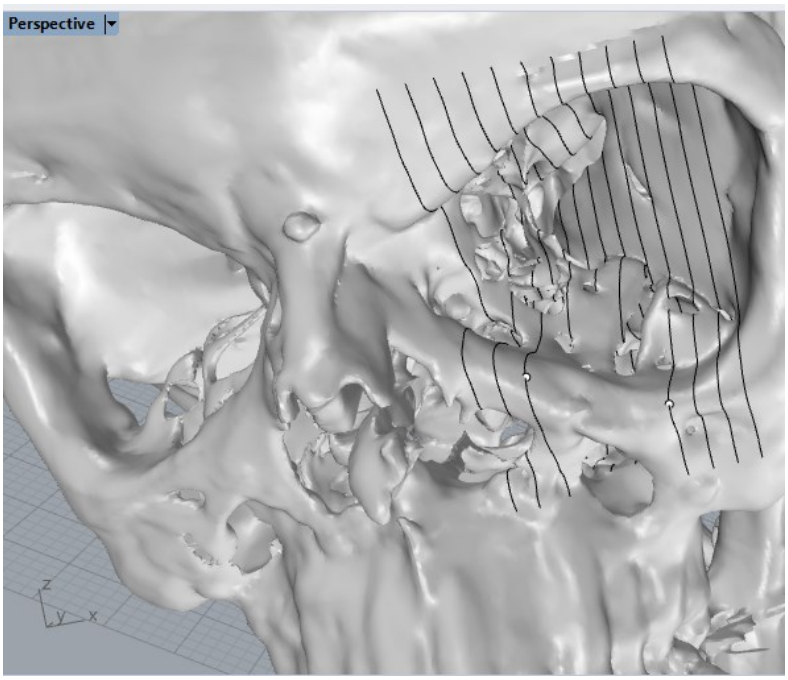

Figure 4.3: Creation of a series of polylines curves.

These curves were used as a baseline for shaping the custom-made implant. The curves were initially irregular, so the quality of the curves had to be improved. It was possible by using the nurbs curves, so curves from control points, selecting a control points for each single curve. At the end, a parallel curve was obtained (Fig. 4.4). Subsequently, the end of these curves was connected to each other using the command "curve interpolate points". Then, this network of curves was used to create the surface of the custom-made implant. In fact, through the command "surface from network of curves" that allow, after selected all curves, to create a patch of surface by considering the four perimeter curves and the internal curves (Fig. 4.5).

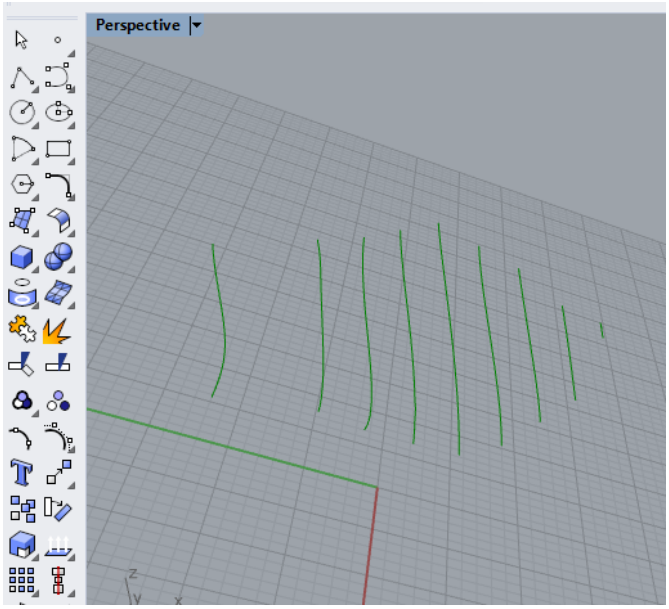

Figure 4.4: Curves from control points to improve the quality of the first polylines curves.

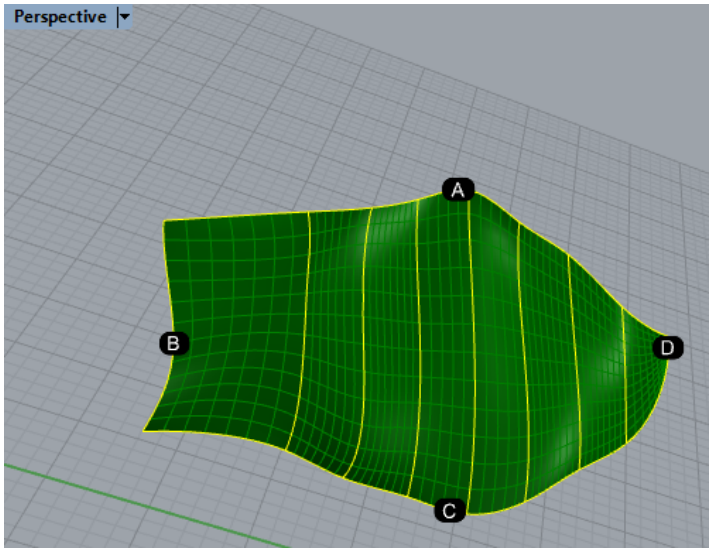

Figure 4.5: Creation of a surface from polylines curves.

The implant was placed in the eye socket and shaped in order to ensure the surgeon to secure the implant into the bone. Next, a protrusion was created so that it could be grasped by the device. This will later be cut out during the operation in order to be fixed inside the orbit.
The last step was to select on the command bar “offset surface” in order to create a solid volume (Fig. 4.6).
Totally, for planning eyeball implant should consider several aspects such as the amount of covering the implant on the basis of kind of fracture and the location of problem, secondly the shape of the implant should be accurately evaluated to warp the implant to the region of the skull defect. The fixation type is another important issue to avoid loosening of the implant.
Loosening of an implant in situ can create specific wear, called fretting which can eventually fail the implant.
To secure the implant plates or screws of proper dimensions can be used according to the material type.
Fixation can also be improved by proper osteointegration of the implant with the bone.

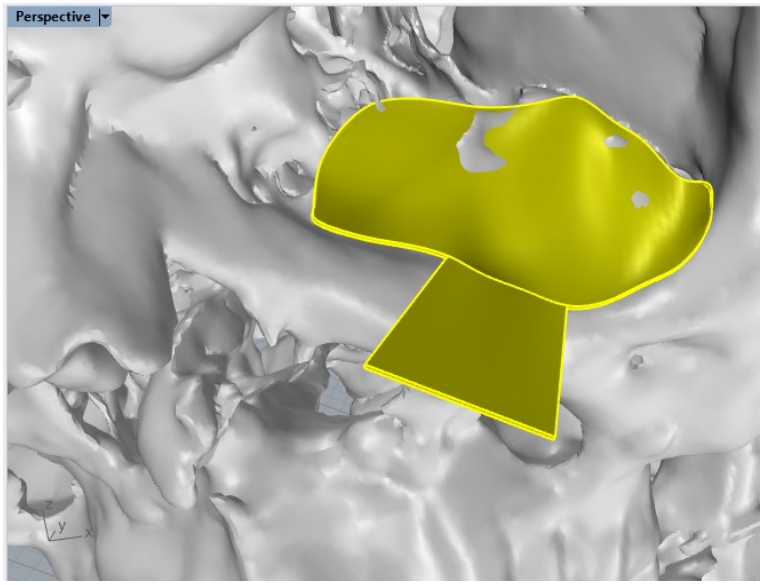

Figure 4.6: Creation of a custom-made implant.

4.2 Modelling the mould

The mould must satisfy several technological and clinical needs to prevent issues with the 3D printing technology and to be successfully used during surgery.

Some important aspects were considered in the design of the mould. Holes have been made on it to insert metal pins. In fact, the mould has been designed to have holes on a box with a depth of 22mm in order to insert the metal pins.

The bespoke implant will be inserted into these metal pins. For this reason, they have been designed to have a pitch of 5.2mm exactly like those present in the implant and with a slightly smaller diameter of 2mm in order to adapt perfectly to the custom-made implant (Fig. 4.7).

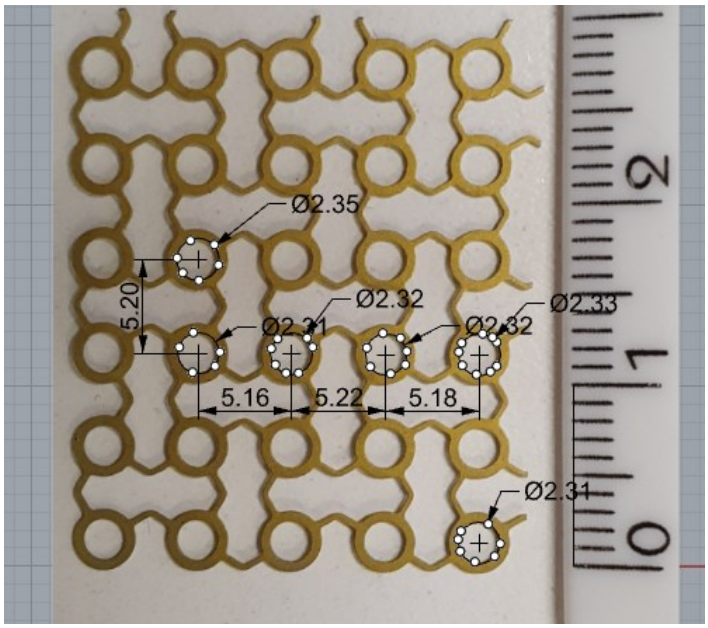

Figure 4.7: Dimensions of the titanium mesh for the case study.

The mould is designed starting from the reconstructed orbital cavity surface as seen in the previuos step using Rhinoceros v.6.29.

The first step was to obtain a solid close polysurfaces from the implant by selecting the command "extrude surface" within the volume command on the lateral bar (Fig. 4.8).

The next step consists in create the base plate.

It was possible through the use, within the command that create a box volume, of a box starting from the center, corner and height.

Then, merge all the curve and extrude them to complete the base and removed the edges by using the command "fillet edges" selecting a radius of 10mm. After having obtained the base and the solid from the surface, with the "Boolean union" command it was possible to join the two solids making them a closed solid polysurface (Fig. 4.9).

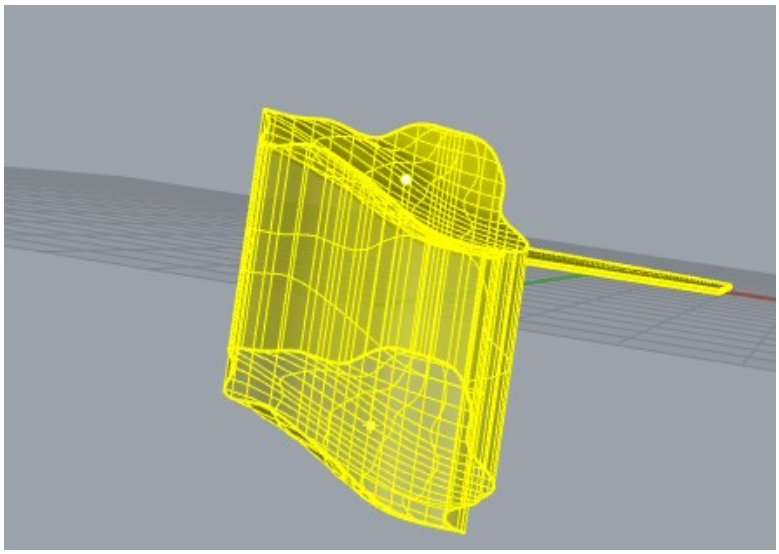

Figure 4.8: Projecting the surface of implant in order to create a solid.

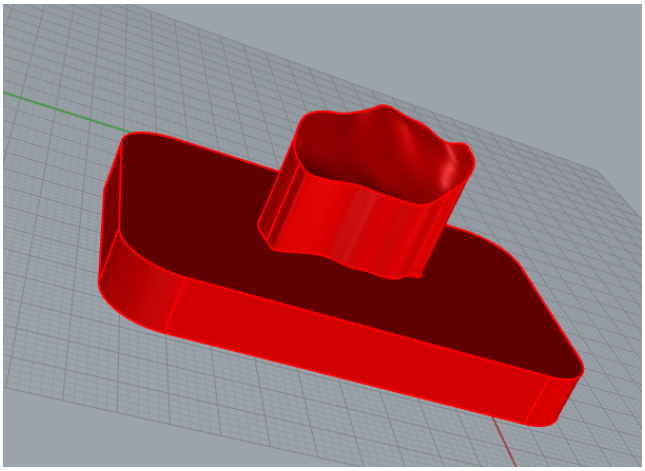

Figure 4.9: Boolean union between the plate e the extruded surface.

To provide stability, a vertical pin was created. In the lateral bar, it was selected the button “cylinder” and the button within the box volume to create a volume starting from center, corner and height. Importantly, a box has been added, in which there are two holes with a diameter of 2.1mm, inside which two metal pins with a length of 22mm and a diameter of 2mm will be inserted, so that the prosthesis remains hooked on they. The distance between the two holes is 5.2mm and represents the distance between two holes of the titanium mesh prosthesis obtained for the case study. For the realization of these holes, two cylinders were created on the surface of the box and through the command "Boolean difference" it was possible to obtain these holes in such a way as to be able to

insert the metal pins later. At the end, to complete the lower mould, all of these elements were joined with the command “boolean union” in order to obtain a closed polysurface (Fig. 4.10).

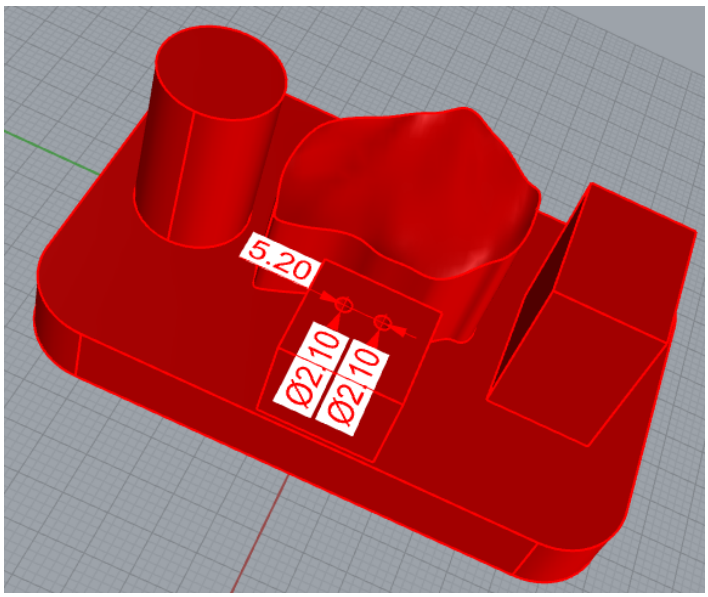

Figure 4.10: Lower mould.

For the realization of the upper part of the mould more or less the same steps have been carried out as those seen for the realization of the lower mould. First of all, starting from the custom-made implant of the previous chapter, with the “extrude surface” command it was possible to create a closed solid polysurface. Subsequently, with the “mirror” command present in the sidebar in the “move box”, it was possible to make a mirror copy of the base and move it to the closed solid polysurface. Finally, with the Boolean union command, the two parts were merged.

For the realization of the cylindrical and rectangular holes which will fit into the two pins of the lower mould, cylindrical and rectangular, several steps have been performed. For the realization of the cylindrical hole, with the command "tube" in the box volume it was possible to create a tube with a diameter of 16.3 mm with a thickness of 3mm and a height of 30mm. For the rectangular one, a rectangle was created starting from the center, vertex and height, same thickness of 3mm and height of 30mm.

Finally, for the creation of the holes in which the pins of the lower mould will be inserted, through the command "extrude surface" and the extrusion of the cylinders it was possible to create the box for the upper mould. The difference was to increase the diameter of the holes in the upper mould by 0.1mm in order to fit perfectly into the lower part. Once all closed solid surfaces have been obtained, with the command "Boolean union" they have been joined (Fig. 4.11).

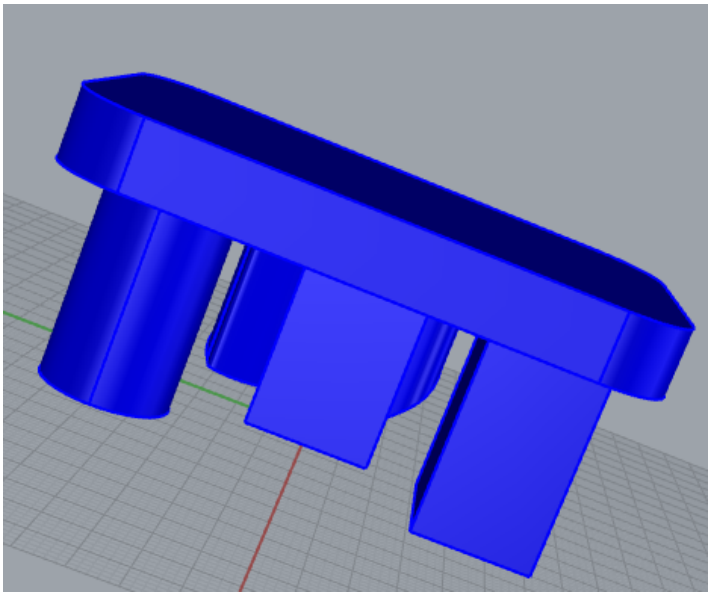

Figure 4.11: Upper mould.

Die and punch shapes have been defined to improve the mould usability. The upper surface of the die has been constructed by projecting of implant boundaries along the directions perpendicular to the extracting one, thus obtaining a large square base. This solution ensures a large contact area to improve stability during the mould usage. The mould guarantees a vertical gap of 5mm between the pins and relative cylinders for modelling implants with different thicknesses (Fig. 4.12). The distance of pins is adjustable which has been determined guaranteeing the possibility to insert the undeformed implant (Fig. 4.13). Furthermore, the pins have been arranged in that point so as not to create problems for the device when the prosthesis is attached.

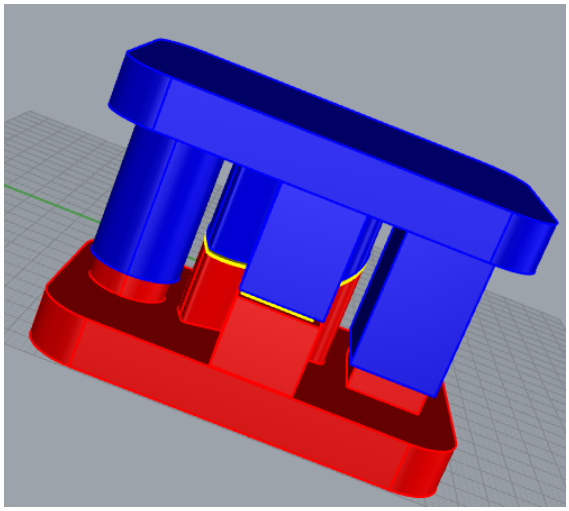

Figure 4.12: Final mould, gap of 5mm between pins and cylinder.

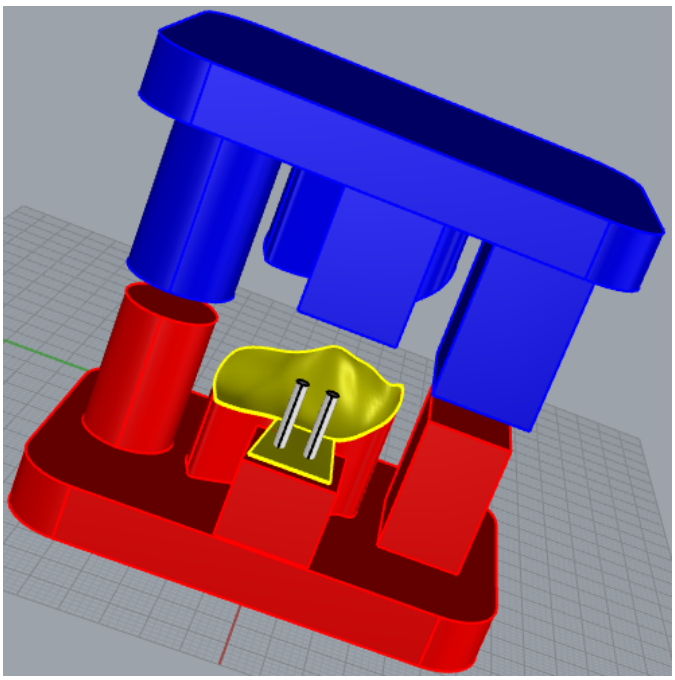

Figure 4.13: Final mould.

4.3 Modelling the medical device

After having made the custom-made implant and the mould, the aim of this study was to design a medical device capable of helping the surgeon to insert a prosthesis in a titanium mesh.

The first step in designing the device was to create on paper a basis of what will then be created on the CAD (Fig. 4.14). The device consists of two parts, one lower and one upper.

It is characterized by the presence of a limit switch device in order to provide the surgeon, during the operation, a feedback for the correct positioning and orientation of the custom-made implant.

There are two pins that have the task of correctly attaching the prosthesis. After having defined a simple diagram of the device on paper, moved on to modeling on CAD.

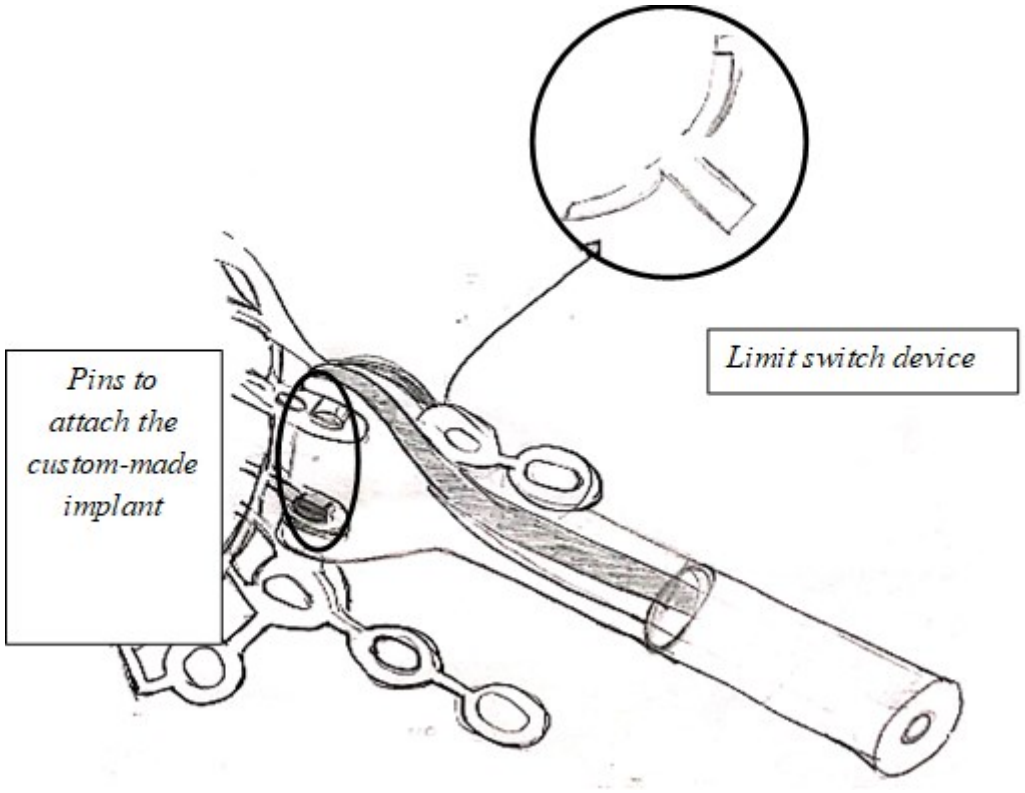

Figure 4.14: Representation of the medical device on paper. There are the limit switch device and the pins useful for hooking the custom-made implant.

Through a careful analysis of requirements, functions and specifications, moved on to CAD design. The device also has been designed used Rhinoceros v. 6.29.

The geometry of the device is very simple. In fact, the device consists of a lower part and an upper part.

The coupling mechanism of the custom-made implant with the device is by grip mechanism. The two parts will be joined by a hinge in such a way as to allow the device to perform only vertical and non-rotational movements.

The presence of a spring is important, as it has the function of bending the upper part of the device in such a way as to close correctly and grasp the custom-made implant.

In the lower part (Fig. 4.15), two 2.1mm diameter pins have been made with a distance of 5.2mm so that the holes of the prosthesis can be inserted correctly and a space in which the custom-made implant will be inserted. To do this, two cylinders were made through the "cylinders" command in the sidebar and through the "Boolean union" command they were joined to the lower part of the device (Fig. 4.16).

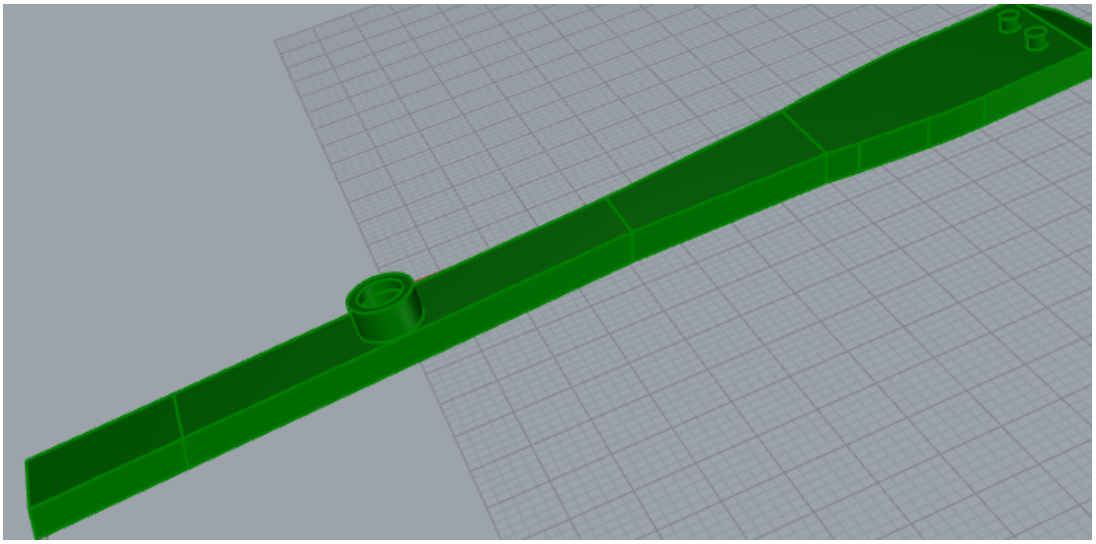

Figure 4.15: lower part of device.

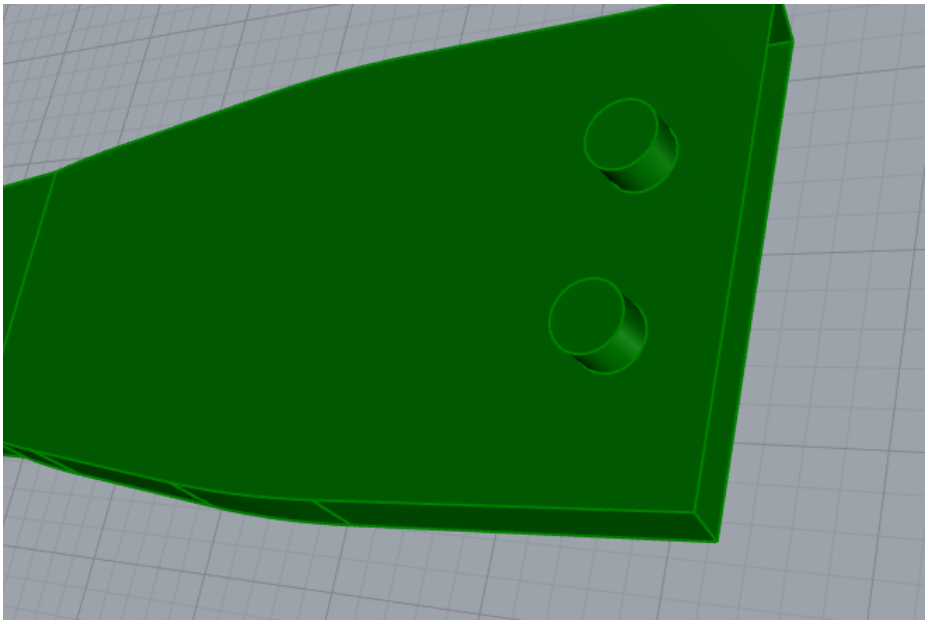

Figure 4.16: Pins of the device.

The top of the device is symmetrical to the bottom. The only difference between the top and the bottom, in terms of geometry, is that the top has a curvature. The latter serves to have a greater grip of the device during the operation (Fig. 4.17). Two 2.3mm diameter holes have been drilled with a 5.2mm spacing so that the top fits into the bottom (Fig. 4.18). As in the lower part, two cylinders were made through the "cylinders" command in the side bar and through the "Boolean difference" command it was possible to obtain the two holes.

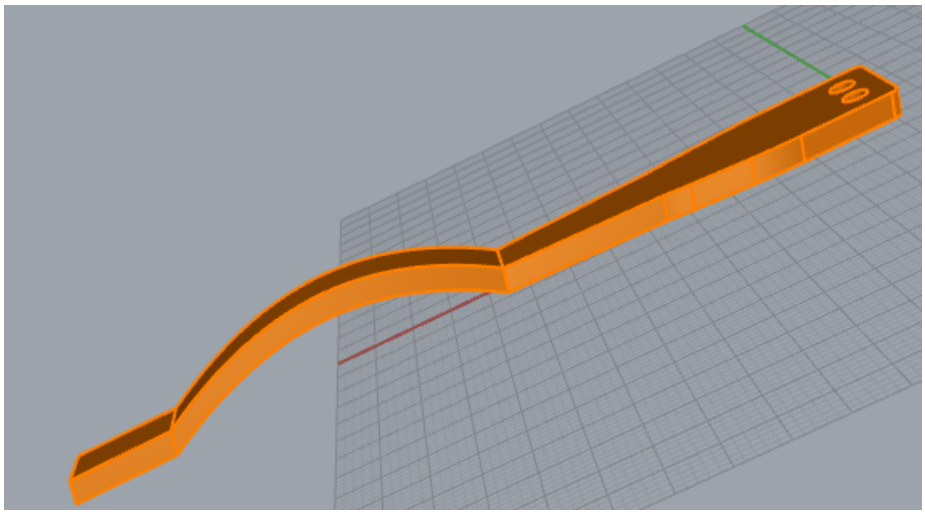

Figure 4.17: Upper part of the device.

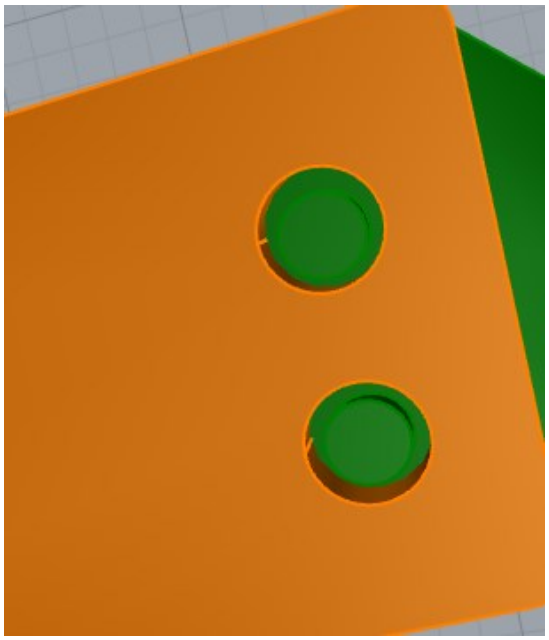

Figure 4.18: Holes of the device.

In the design of the device three important aspects were taken into consideration. The first concerns the design of a "limit switch" device. The latter has the purpose of indicating to the surgeon the arrival on the orbital edge in order to orient the device and insert the custom-made implant correctly. Furthermore, this device must be designed each time according to the orbital edge of the patient who will be operated on. As for the creation of the curves to define the geometry of the custom-made implant seen in section 4.1, curves have been defined on the orbital edge (Fig. 4.19). These curves were used as a baseline for the realization of a “limit switch”. Then, this network of curves was used to create the surface of the custom-made implant. In fact, through the command “surface from network of curves” allow, after selected all curves, the creation a patch of surface of the “limit switch” (Fig. 4.20).

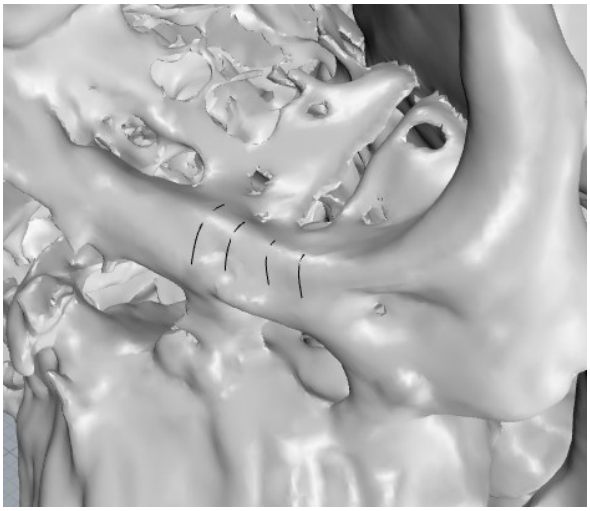

Figure 4.19: Polylines curve on the orbital edge.

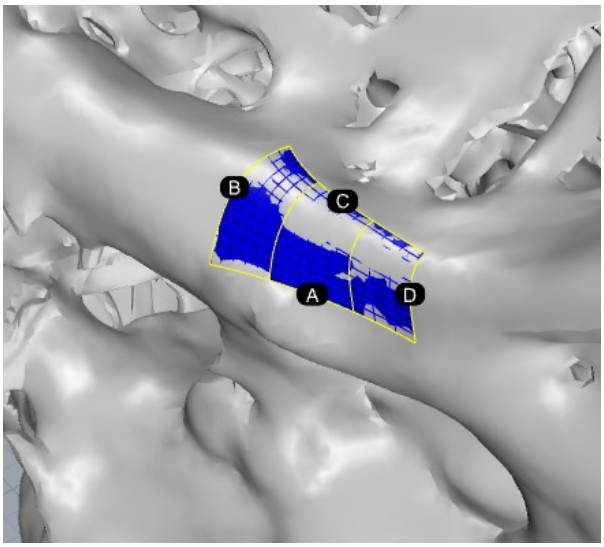

Figure 4.20: Realization of the surface of the “limit switch device”.

Where having created the surface, through the command "extrude surface" it was possible to obtain a solid (Fig. 4.21). Finally, to anchor it to the device, two holes have been made so that it can be hooked to the device. Two pins have been made at the base of the lower part of the device, while two holes in the limit switch device, executing the "Boolean difference" command (Fig. 4.22). The other two important aspects for the design of the device were the insertion of a spring and the insertion of a hinge at the end (Fig. 4.23). The first helps the device to flex to hook the custom-made implant with a grip mechanism, while the second serves to allow the device only vertical movements. At the end of all this design, the device will consist of an upper and a lower part (Fig. 4.24). The two parts will then be hinged together in such a way as to provide only vertical movements to the device and not rotational. The spring will be present in the center to ensure greater flexibility to the device and to allow the upper part to join the lower part and hook the custom-made implant. In addition, two CAD models were created. The first is that of the prototype to be brought to print while the second will be the commercial prototype. The difference between the two is that the first will be printed using the SLS technique and will be in polyamide while the second will be printed in steel. Furthermore, another difference lies in the construction of the limit switch. In the one printed using the SLS technique, the limit switch device is joined to the lower part of the device while in the second it is a custom device and will be made each time according to the patient's orbital edge.

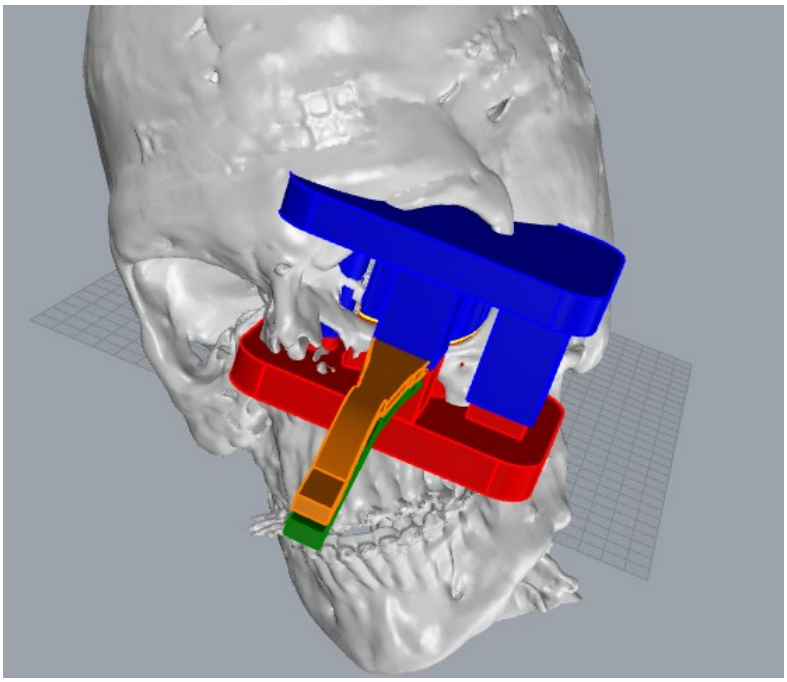

Figure 4.21: Realization of the surface of the "limit switch device".

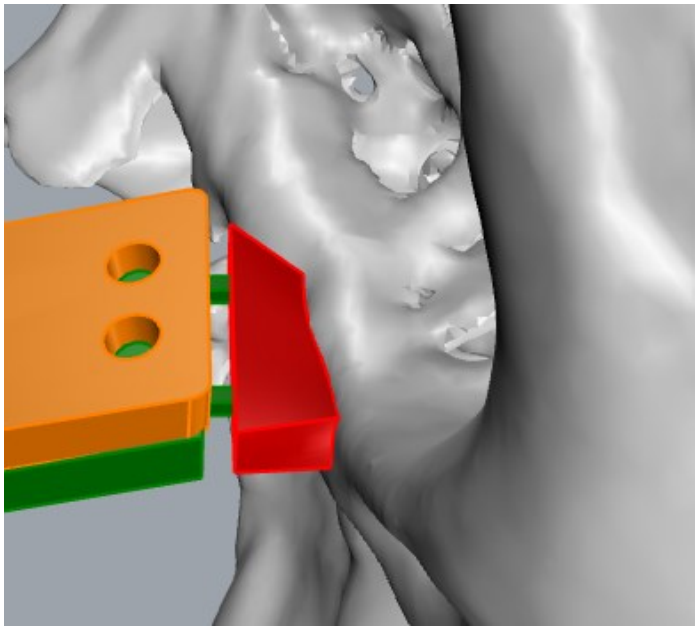

Figure 4.22: "Limit switch" device.

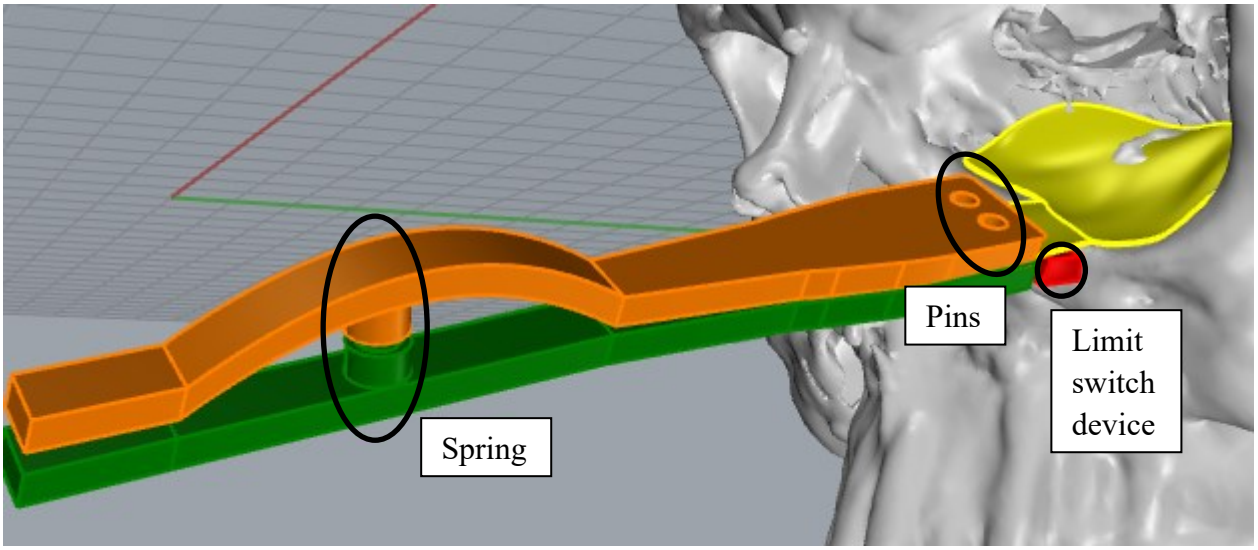

Figure 4.23: Final device.

Figure 4.24: Use of the device in the operating room.

5-RESULTS AND DISCUSSION

5.1 Final mould

After the design on Rhinoceros, the mould and the medical device has been manufactured in polyamide using the Selective Laser Sintering technique (Fig. 5.1). As introduced in section 3.2, the mould must satisfy some mechanical and clinical requirements.

A fundamental requirement is that the mould be sterilizable because it must be used in the operating room. This requirement is satisfied as the objects produced by SLS are sterilizable.

The advantages of using the SLS technique are that the objects made are cheap, easy and quick to make, have high precision, durability and are made of a versatile material. For this reason, other clinical requirements are satisfied. Another problem concerns the deformation of the titanium prosthesis.

This problem is due to the fact that when the prosthesis is deformed, by loosening the pressure on it, there will be an elastic return causing the prosthesis to not fully deform.

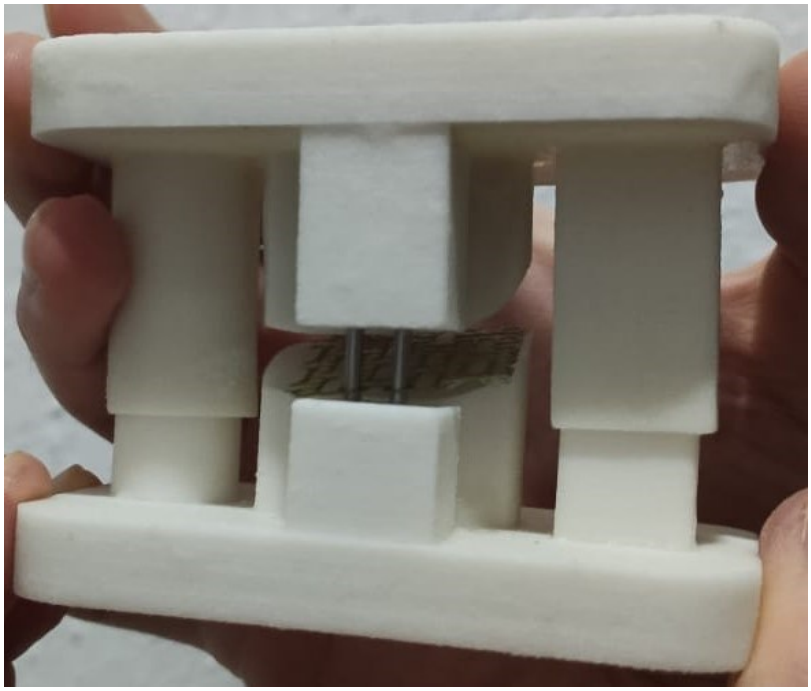

Figure 5.1: Mould manufacturing using SLS technique.

A problem in making the mould concerns the two pins. These pins have the task of giving stability to the structure. They were made with a thickness of 2mm, due to this, at the end of the manufacturing process, the edges were subject to breakage (Fig. 5.2).

The holes in which the metal pins were inserted, were made with the right distance of 5.2mm and with the right diameter.

A small disadvantage in processing with the SLS technique is that residues of dust may remain in the holes, this would cause an occlusion of the same.

Mechanical requirements have been satisfied, such as the mould dimension must be minimal, the coupling tolerances on the different parts of the mould must be suitable for the additive manufacturing process and so on. A problem arises in tolerance regarding the insertion of the prosthesis. Pins with a diameter of 2.3 mm have been made, for this reason the prosthesis tends to perform rotational movements (Fig. 5.3).

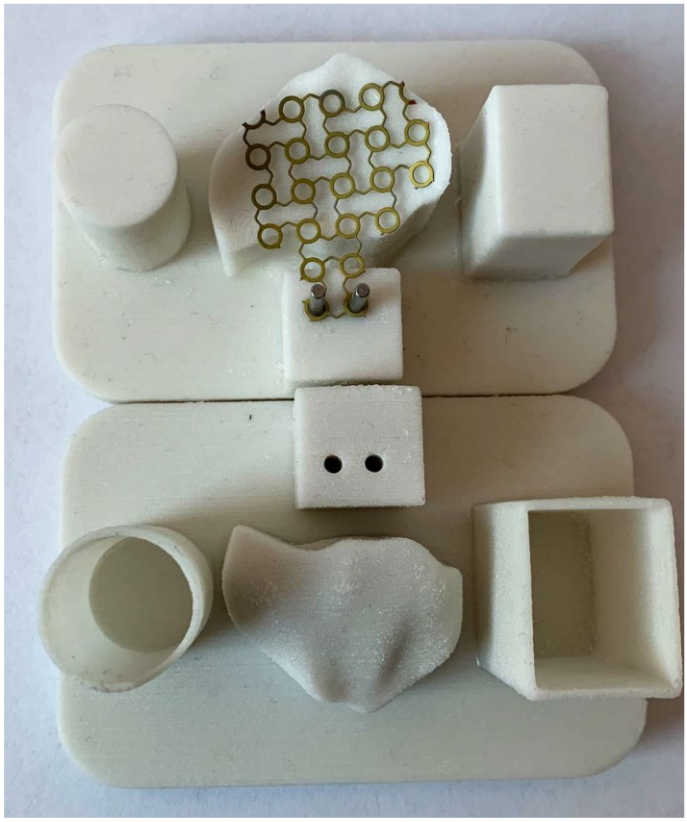

Figure 5.2: Top and bottom of the mould. The two metal pins useful for inserting the prosthesis are visible. Furthermore, the thickness of the two side guides is clearly visible.

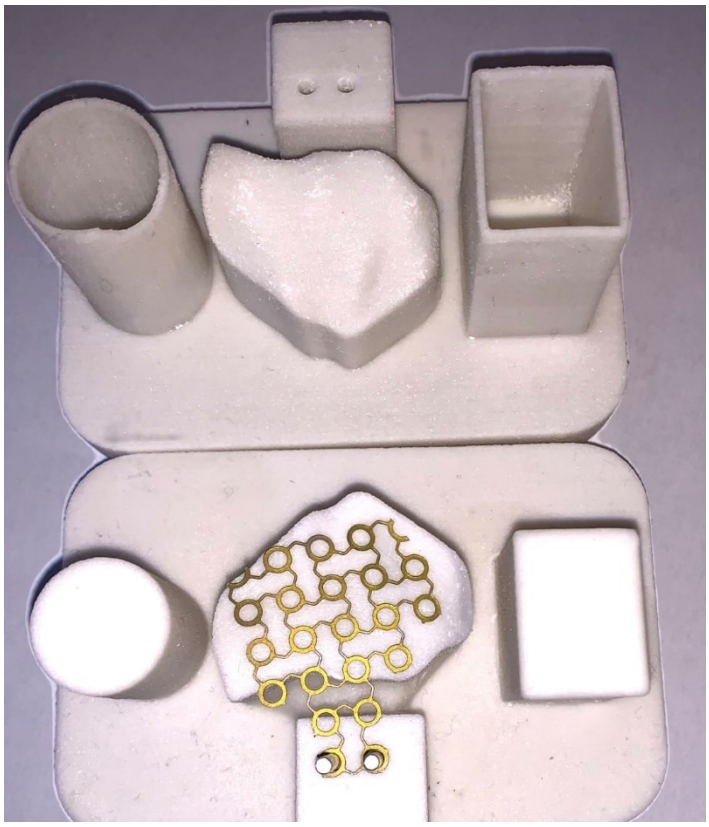

Figure 5.3: Coupling tolerances on the different parts of the mould.

As for the prosthesis, once deformed, it was easily cut with scissors in such a way as to have the shape of the orbital cavity of the case study (Fig. 5.4).

Figure 5.4: Deformed and cut prosthesis.

5.2 Final device

The aim of this study was to design a medical device capable of helping the surgeon to insert a titanium mesh prosthesis in a fractured eye socket, trying to highlight what could be the advantages and disadvantages compared to classical instruments used in surgery, also the verified requirements are showed in the table VII.

As well as the mould, the device was made of polyamide using the SLS technique. The results show that the device satisfied most of the requirements.

It is certainly sterilizable, having been made with the same material as the mould. SLS has been selected for the following advantages:

- Possibility to manufacture autoclave sterilizable parts;
- Small series produced in one manufacturing process;
- Fast and economical process;
- Functional;
- No supports required;
- All kinds of finishing degrees;
- High accuracy;
- Durable;
- Material versatility.

Being sterilizable, the device is usable in the operating room. Having a simple geometry, it is easy to use and is ergonomic (Fig. 5.5). The limit switch device provides the surgeon with correct feedback for the correct positioning and orientation of the custom-made implant. The spring allows the device to hook and unhook the implant correctly. Being molded in polyamide, the device completely fulfills the requirement of low cost.

Furthermore, the manufacture of a mould and the device through the SLS technique allows to reduce the duration of the operation.

The device is reusable and can be used to treat patients with orbital floor fractures.

One requirement in particular was not satisfied.

The device has been designed to be used for deformed prostheses. The titanium mesh is easily usable with the device while the demineralized bone plate is not usable. This is a first disadvantage of the device.

AIM	REQUIREMENTS	VERIFIED
1.To choose the correct material	Biocompatible material	Yes
2.Economic benefit to the patient	Low cost	Yes
3.To introduce the device in the operating room	Device must be Sterilizable	Yes
4.To use the device several times	Reusable	Yes
5.To be secure	Ergonomic	Yes
6. To orient unequivocally and easily the device during the surgery	Easy to use	Yes
7.To choose the implant material during surgery	Usable for deformation prostheses	No, device can be used only for titanium mesh prosthesis
8. To treat orbital fractures	Suitable for orbital floors and walls	Yes

Table VII: Verified requirements.

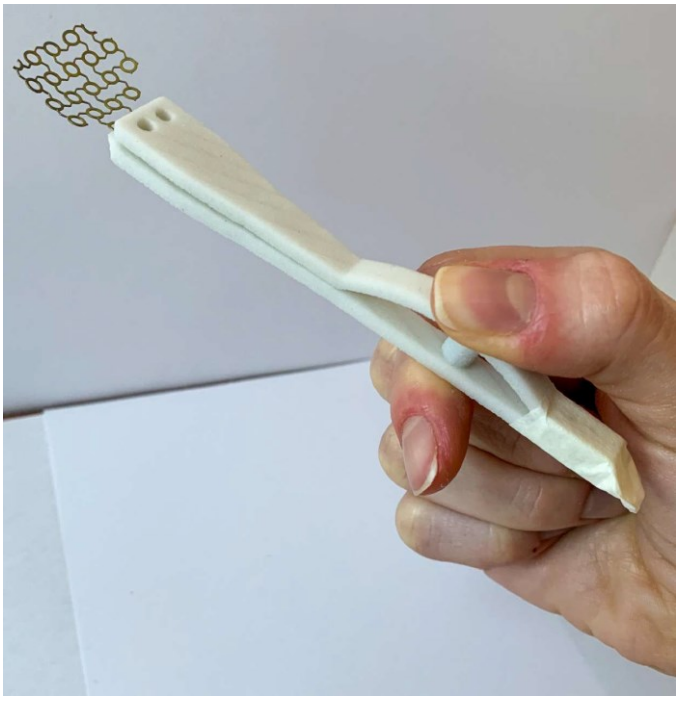

Figure 5.5: Medical device. The ends of the bottom and top are hinged. Visible is the curvature of the upper part of the device allowing easy use.

Furthermore, some fundamental aspects have been highlighted in the functionality of the device (Table VIII). The first is to provide the surgeon with feedback for the correct orientation and positioning of the prosthesis.

This was done correctly by designing the limit switch device in the CAD. The limit switch device was created by following the orbital edge of the case study.

This will allow the surgeon to position himself correctly with the device on the orbital rim and to insert the prosthesis.

In the commercial prototype, the limit switch device must be made each time as each patient has a different orbital edge. In the printing process, in order to verify usability and usefulness, the limit switch was joined to the lower part of the medical device (Fig. 5.6).

Category	**Specification**	**Unit of measure**	**Minimum value**	**Maximum value**	**Value**	**Verified**
Geometry	Dimension control / dimensional tolerance	mm	0	0.5	-	Yes
Materials	Resistant to electromagnetic disturbances	-	-	-	Yes	Yes
User signal	Correct positioning / orientation feedback	-	-	-	Acoustic / Visual	Yes
Security	Uncertainty / accuracy of positioning / orientation	mm	-	-	0.5	Yes
	Need to recalibrate the device	-	-	-	No	No necessary
Production	Productive process	-	-	-	3D printing Sintering	Yes, SLS technique
	Assembly by means of quick couplings	-	-	-	Yes	Yes, easy to use
Economy	Cost	-	0	100	-	2-10€

Table VIII: Verified specifications.

Figure 5.6: Limit switch device. Printed using the SLS technique, it was joined to the lower part of the device and has the task of tracing the orbital edge of the case study.

5.3 Improved mould and device

A problem concerns the deformation of the titanium prosthesis.

This problem is due to the fact that when the prosthesis is deformed, by loosening the pressure on it, there will be an elastic return causing the prosthesis to not fully deform.

This problem can be solved by inserting another box in the mould, opposite to the first, so that the prosthesis can be inserted in the axes of the two holes of the two boxes in such a way as to avoid elastic return (Fig. 5.7) (Fig. 5.8).

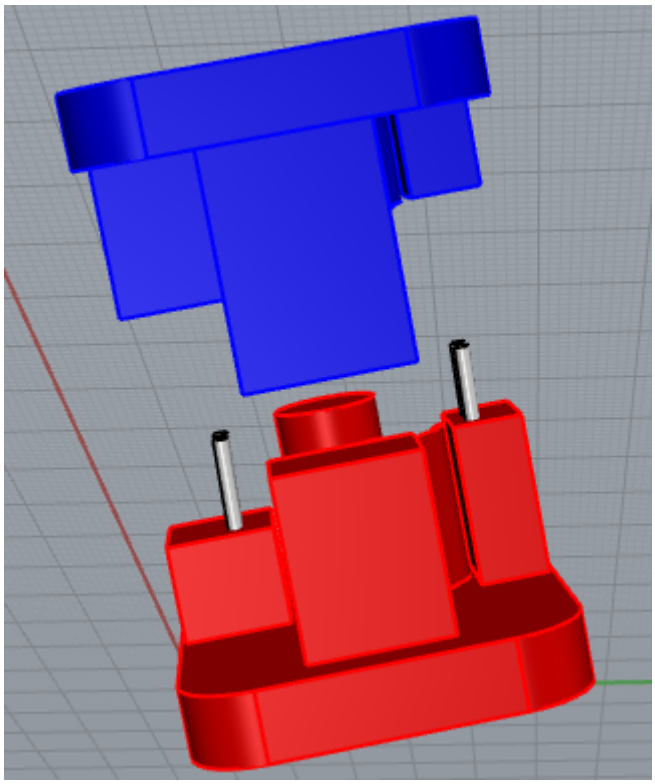

Figure 5.7: CAD representation of the improved mould.

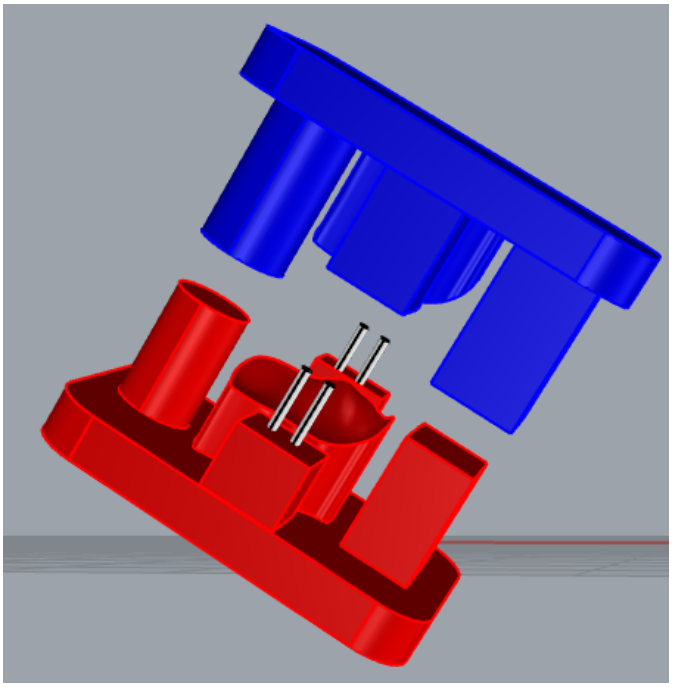

Figure 5.8: CAD representation of the improved mould.

The prosthesis attachment and release mechanism are of the grip type. The pins made in the device have been made correctly.

A problem arises in tolerance regarding the insertion of the prosthesis. Pins with a diameter of 2.3 mm have been made, for this reason the prosthesis tends to perform rotational movements.

This problem can be easily solved by changing the diameter of the two pins.

Another problem concerns the hinge at the end of the device. In the commercial prototype, the top and bottom of the device are joined while the one made in this study are separate.

To improve the correct insertion of the prosthesis inside the orbital floor, the limit switch has been modified.

The choice is due to the fact that, once printed, the limit switch did not guarantee a correct grip on the orbital edge.

For this reason, it was decided to create a limit switch almost double the first in order to completely trace the orbital edge (Fig. 5.9) (Fig. 5.10).

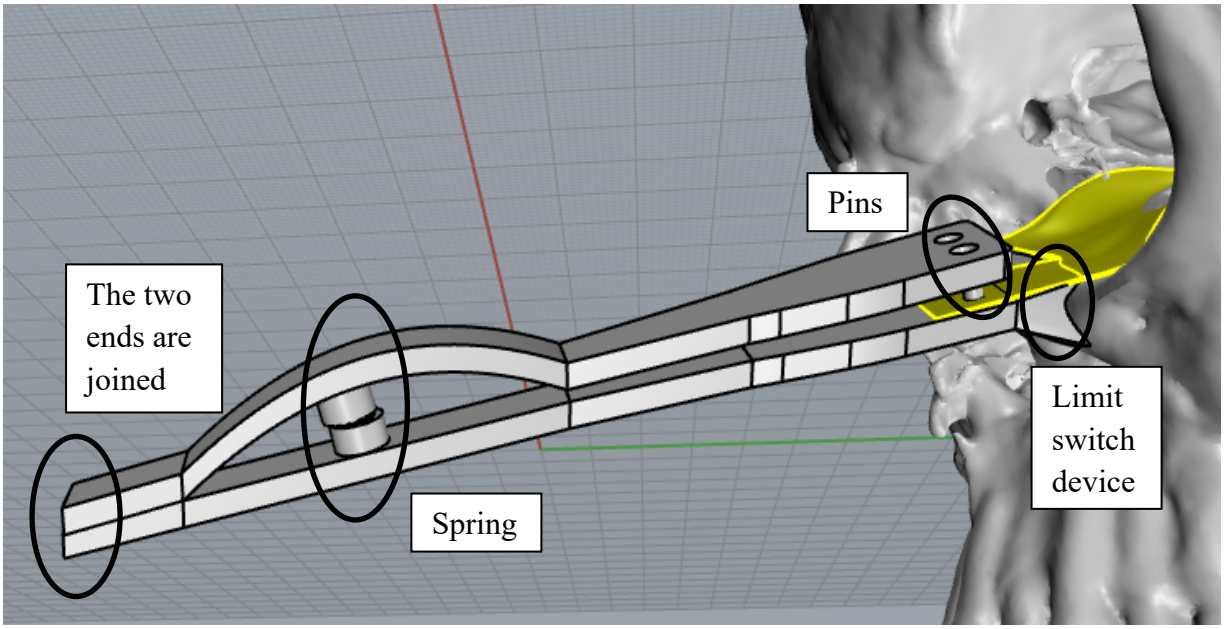

Figure 5.9: Final device.

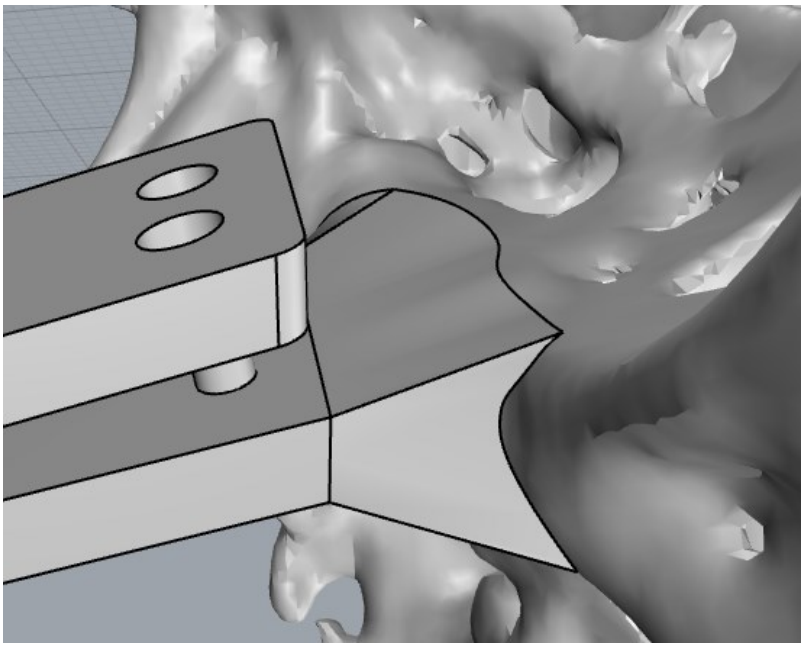

Figure 5.10: Limit switch device.

5.4 Validation of the device and results

The accuracy of the device in positioning the prosthesis and the margin of error with respect to the CAD model were analyzed using the CloudCompare software.

It is a 3D point cloud processing software (such as those obtained with a laser scanner). It can also handle triangular meshes and calibrated images. CloudCompare provides a set of basic tools for manually editing and rendering 3D points clouds and triangular meshes.

It also offers various advanced processing algorithms, among which methods for performing:

- Projections (axis-based, cylinder or a cone unrolling);
- Registration;
- Distance computation (cloud-cloud or cloud-mesh the nearest neighbor distance);
- Statistics computation;
- Segmentation (connected components labelling);
- Geometric features estimation (density, curvature, roughness, geological plane orientation);

To verify the accuracy of the device with that in the CAD model, three tests were performed.

The first step was that, through a laser scanner, to obtain real images of the three tests of the positioning of the prosthesis inside the skull of the case study with the device and then bring them to CloudCompare.

Next, the .stl files of the skull and the reference device were imported to compare the accuracy of the tests performed with the CAD models. The first procedure to be performed was to align the reference skull with that of the test. To perform this procedure, three reference points were placed on the test skull and three reference points on the skull through the command “Align two clouds by picking equivalents point pairs” as shown in the figure 5.11. To have greater precision in the alignment of the two skulls, the “finely registers already aligned entities” command was performed, and this procedure was performed for all three tests (Fig. 5.12).

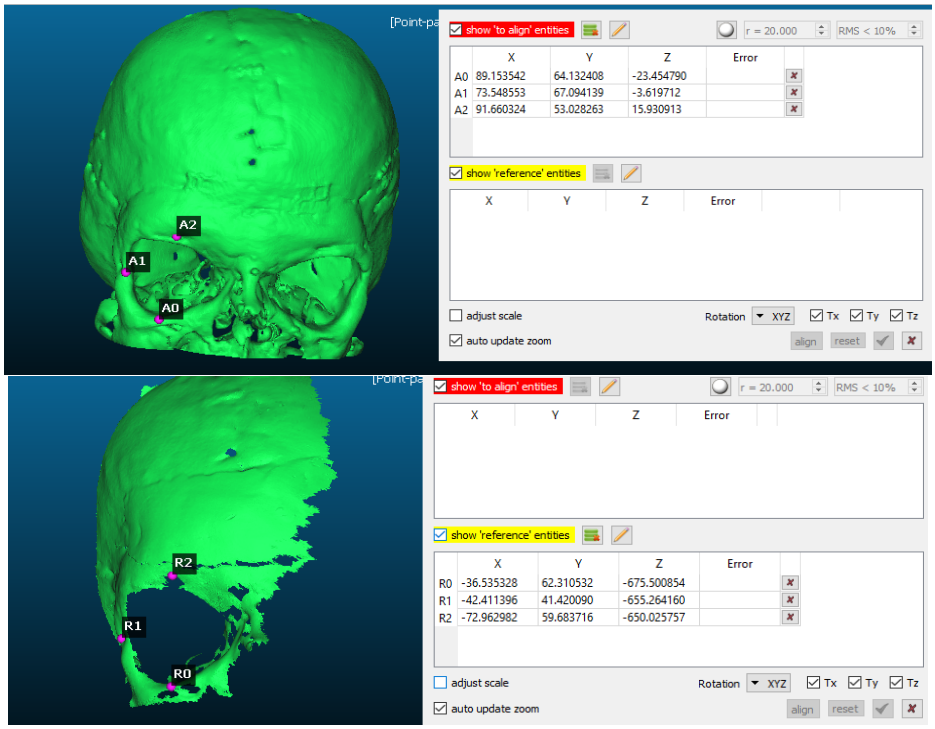

Figure 5.11: Reference points on the skull test and reference skull.

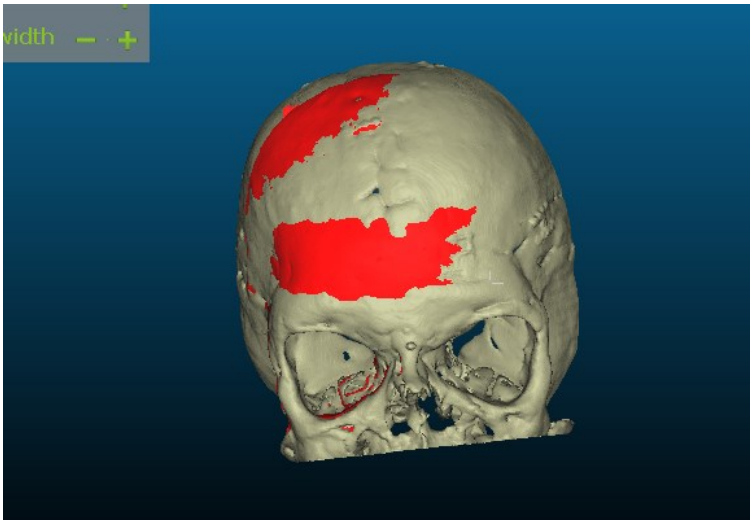

Figure 5.12: Alignment of the two skulls.

After performing the alignment, the next step was to orient the device used in the test with the reference skull. This procedure was performed for all three tests in order to analyze the orientation of the device used in the tests with that present in the CAD model (Fig. 5.13).

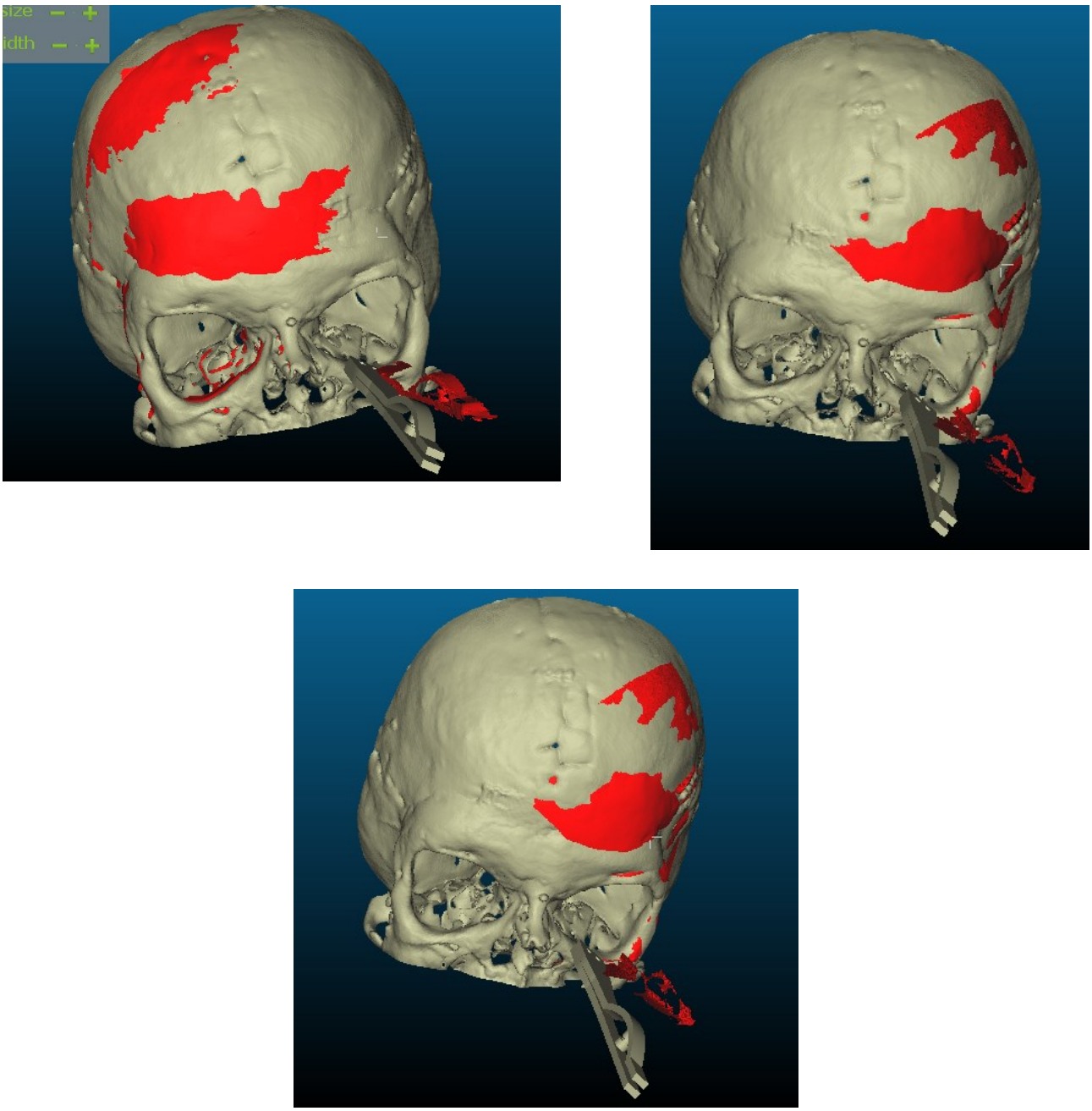

Figure 5.13: Alignment of the trial fixture on the reference skulls for each trial.

After orienting the skull and the device with the CAD models, the last step was to return the .stl files to Rhinoceros to accurately analyze the positioning accuracy of the tests performed against the CAD models (Table IX). The results of the three tests show how the angle of the device changes compared to the reference one.

In fact, from the first test, the angle of inclination is about 8.76 ° with a displacement of about 8.97mm.

The second and third tests were performed by changing the angle of the skull and the device relative to the laser scanner. For this reason, the angle and the displacement of the second and third tests are respectively 17.33 ° and 5.97mm, 19.33 ° and 8.63mm (Fig. 5.14), (Fig. 5.15), (Fig. 5.16).

	Angle	**Displacement**
Trial 1	8.76°	8.97mm
Trial 2	17.33°	5.97mm
Trial 3	19.33°	8.63mm

Table IX: Inclination and displacement of a device with respect the CAD model.

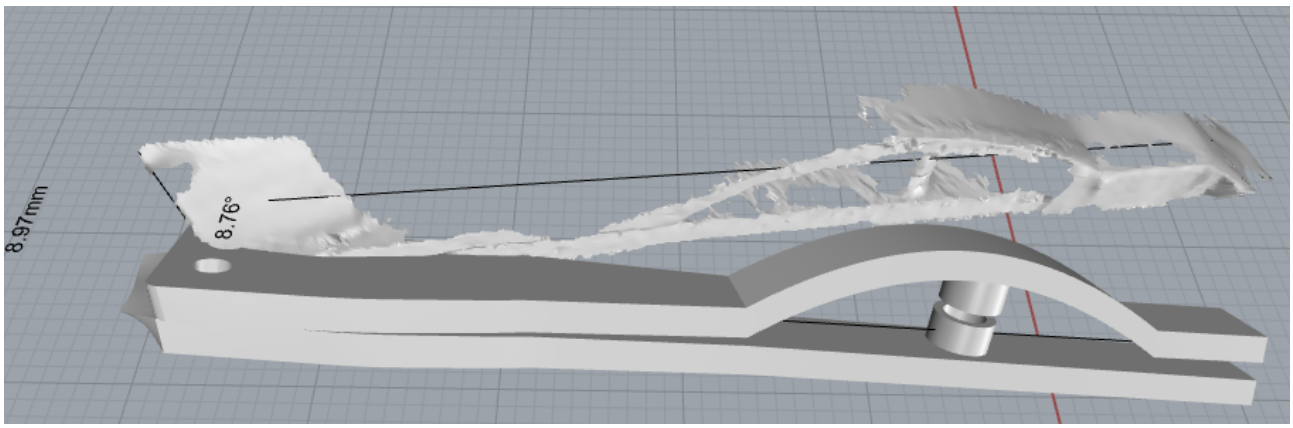

Figure 5.14: Inclination and displacement of the first trial.

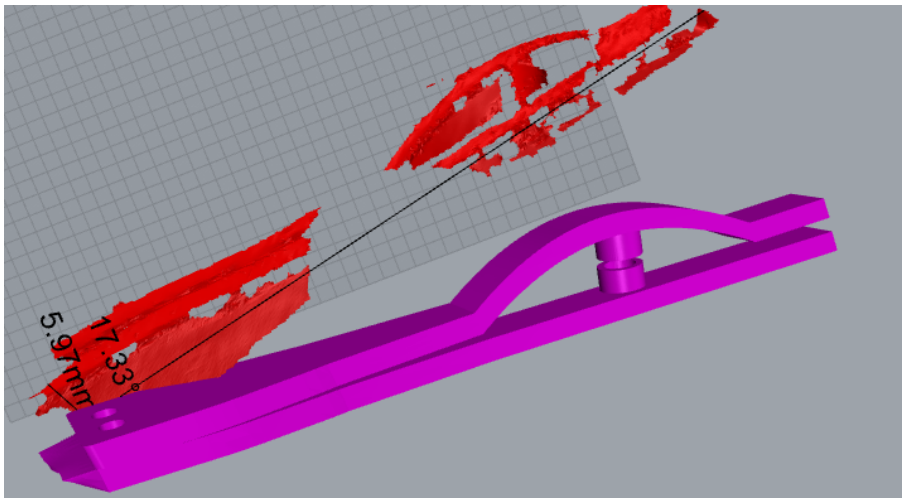

Figure 5.15: Inclination and displacement of the second trial.

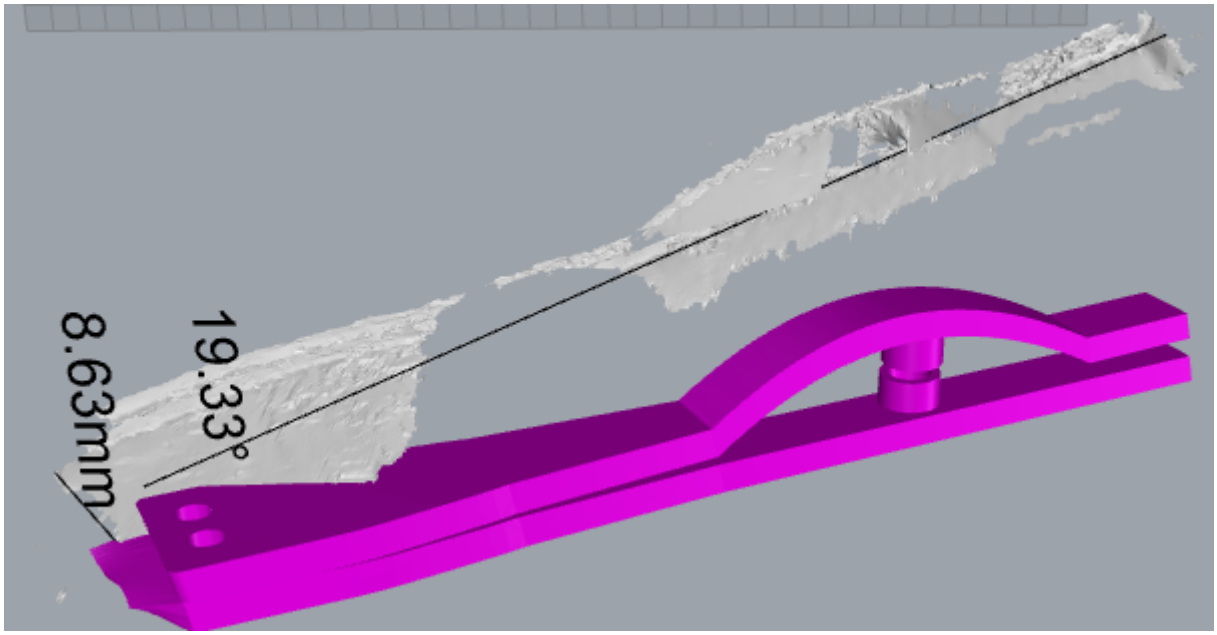

Figure 5.16: Inclination and displacement of the third trial.

The same procedure was performed to analyze the deformation of the prosthesis and how much the elastic return has suffered compared to the modified CAD model. The deformed prosthesis was then scanned with the laser and reported on CloudCompare. Through the three-point alignment it was superimposed on the reference one. The results show how the prosthesis does not differ from the reference one, as regards the elastic return, having a difference of about 0.23mm as shown in the figure 5.17.

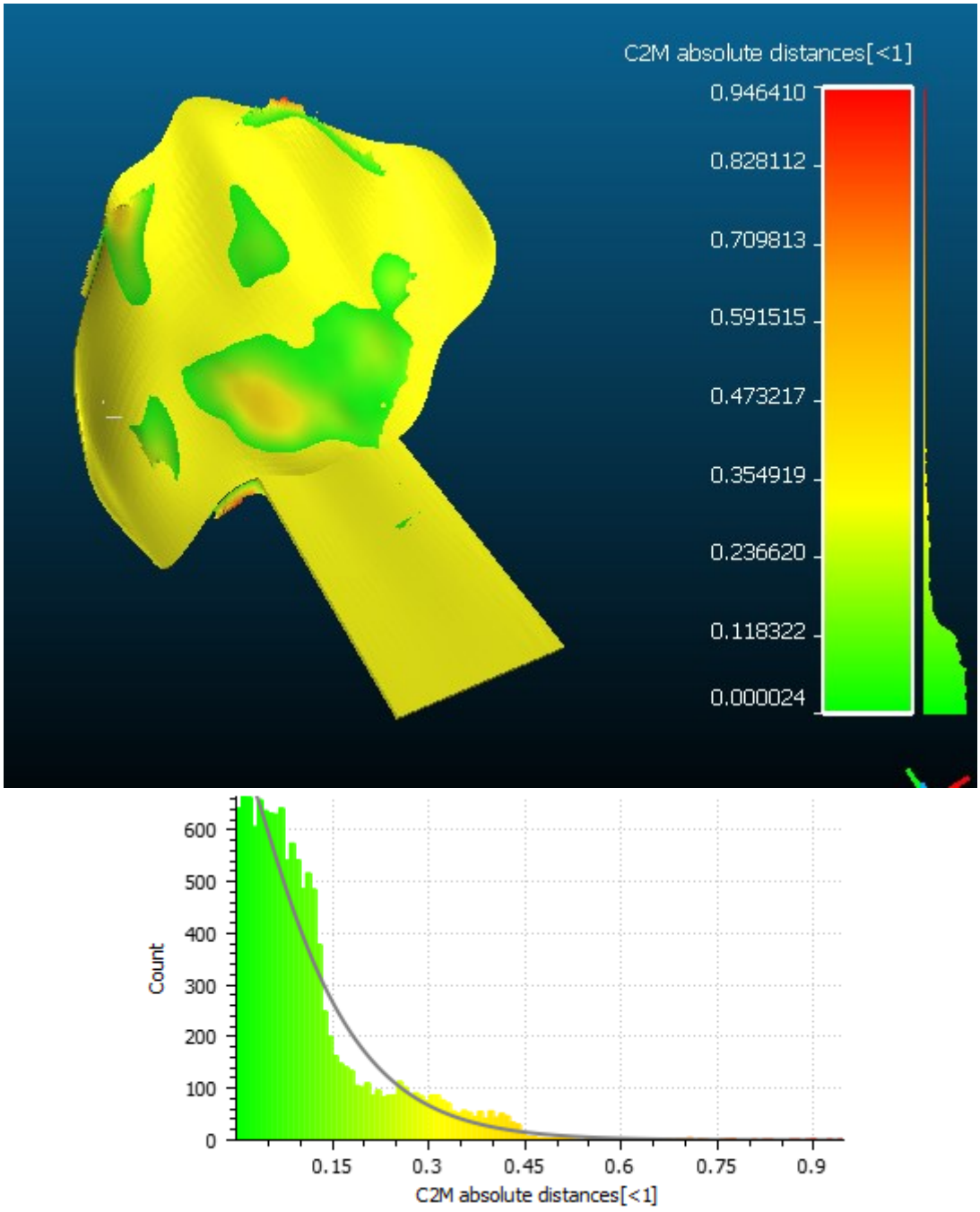

Figure 5.17: Align the deformed prosthesis with the CAD model. On the right it is possible to see a scale that indicates in green a minimum alignment error and red the maximum.

The last step was to fully verify the accuracy in positioning the deformed prosthesis within the ocular orbit in order to define how much the positioning error was compared to the CAD model. To verify the accuracy in positioning the prosthesis correctly inside the orbital cavity, the same procedures previously illustrated were performed. After scanning the test skull with the device and the prosthesis correctly inserted (Fig. 5.18), the files were imported to CloudCompare. Subsequently, after aligning the skulls, the prosthesis was positioned relative to the one in the CAD model (Fig. 5.19).

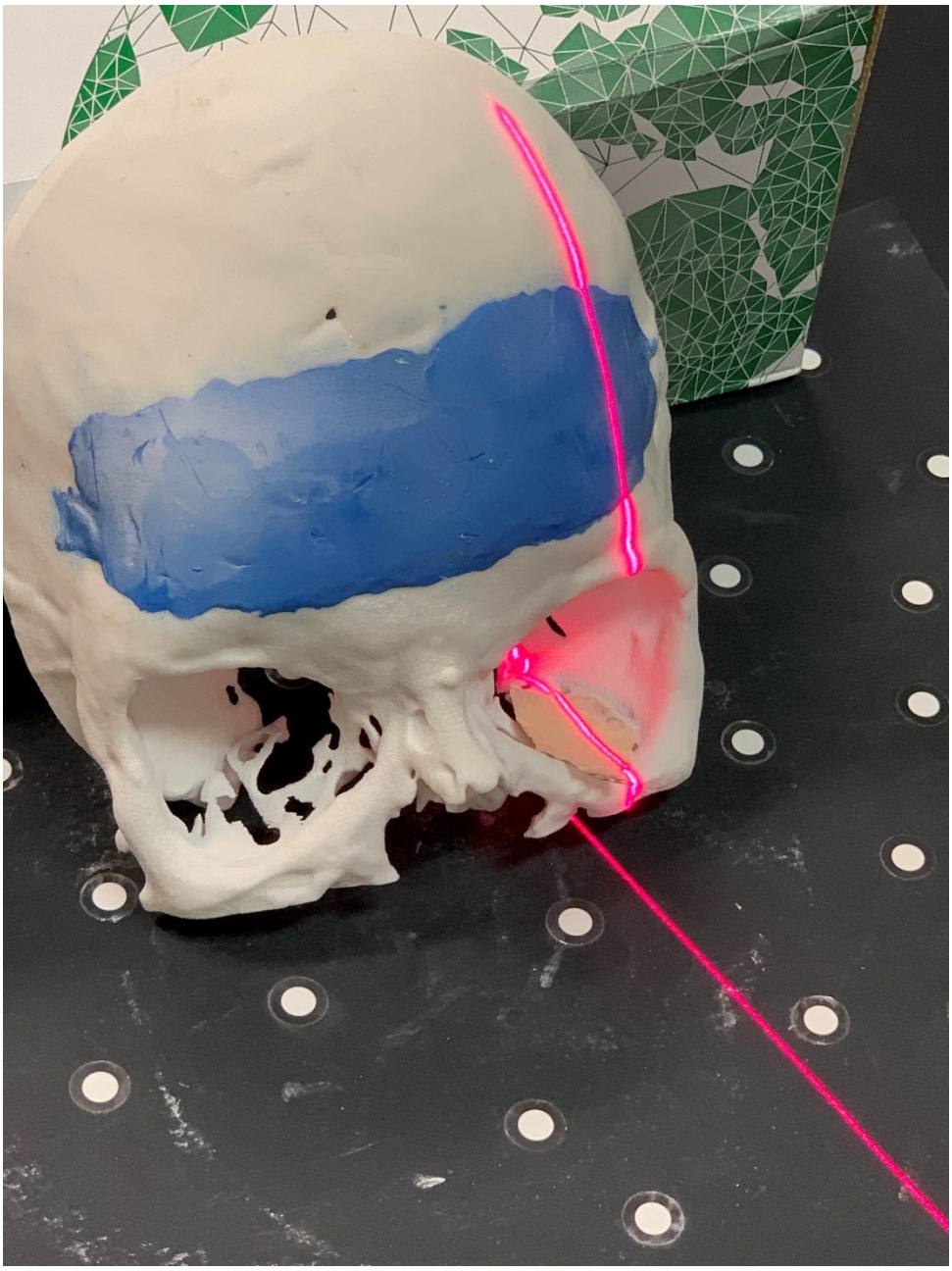

Figure 5.18: Scan of the skull and the prosthesis correctly inserted.

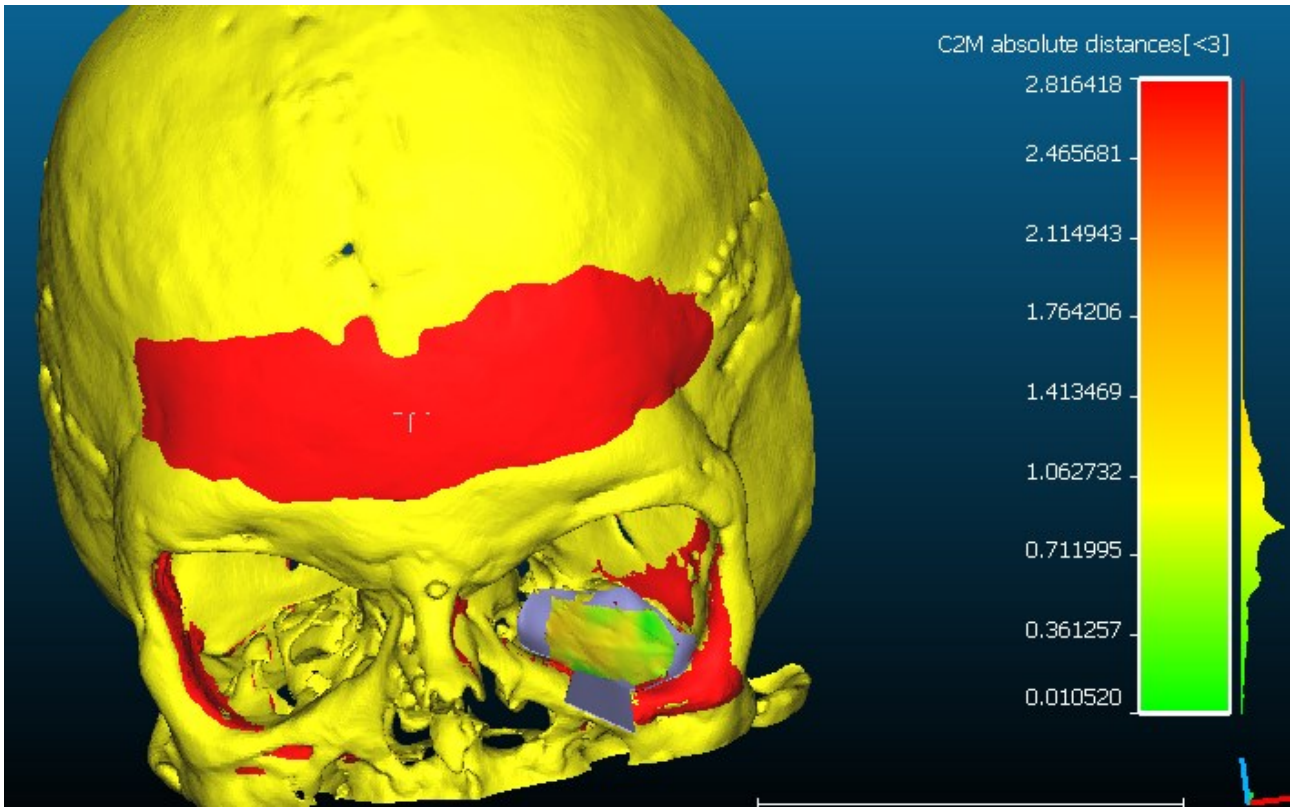

Figure 5.19: Insertion of the prosthesis on the reference one on CloudCompare.

The results show that the prosthesis inserted through the device into the skull does not completely deviate from the prosthesis designed on the CAD model. As shown in figure 5.20, it is possible to notice a gauss curve showing a deviation level equal to 0.84mm. This result is certainly important but to be analyzed.

In fact, to perform the test, the prosthesis was coated with a layer of adhesive tape as the same, being perforated, was not completely scanned by the laser.

Furthermore, another aspect to consider is that the prosthesis must be fixed inside the orbital cavity with one or two screws.

For this reason, the deviation from the CAD model is minimal and this demonstrates how the requirements such as the use of the device to treat orbital fractures have been met.

Furthermore, the function of the device to correctly position the prosthesis and to provide feedback of the correct orientation of the device via the stop has been demonstrated.

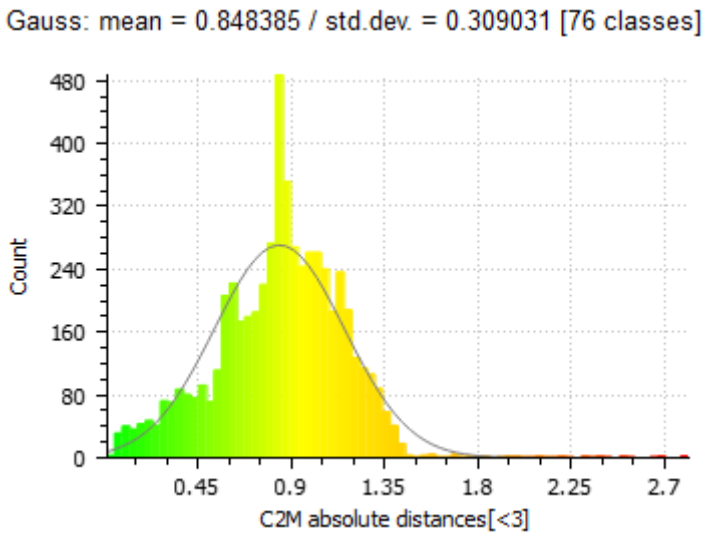

Figure 5.20: Gauss curve showing the deviation of the prosthesis of 0.84mm compared to that of the CAD model.

6-CONCLUSIONS

Reconstruction of orbital cavities defects is a very delicate surgery and difficult to perform and complications are mainly due to difficulties in restoring orbital anatomy and volume. Appropriate management of these injuries avoids diplopia, enopthalmos dystopia, and abnormal facial appearance. The use of high-resolution computed tomography (CT), with the ability to examine the scans routinely in three planes, has provided a better understanding of the three-dimensional (3D) structure of the bony orbit. The success of reconstructive orbital surgery depends on diverse aspects of the preoperative evaluation of the defect, the design and manufacturing of the implant and the execution of surgery. In fact, prefabricated patient-specific implants, designed using a patient's computed tomography (CT) data to precisely restore the missing anatomy, are increasing in popularity as a surgical solution for these more complex orbital defects.

These implants reduce surgical complexity, decrease operative times, minimize exposure and risk of contamination, and have resulted in improved cosmesis and patient satisfaction. During the past decades, autogenous bone grafts were considered ideal for the treatment of orbital floor fractures. Titanium mesh and high-density porous polyethylene implants are presently the most commonly used nonresorbable synthetic allopastic materials for orbital floor reconstructions, also are easier to handle and offer the possibility of obtaining a precise three-dimensional (3D) reconstruction. The aim of this study was to design a medical device capable of helping the surgeon to insert a titanium mesh prosthesis in a fractured eye socket, trying to highlight what could be the advantages and disadvantages compared to classical instruments used in surgery. The first step to start the design and production process of the implant and the medical device was the acquisition of the scan images (CT) of the computed tomography (CT) first in the Mimics software and then in Rhinoceros v.6.29, subsequently the realization of custom-made implant, the relative mould and then, the medical device. The sterilized SLS mould could be used during orbital surgery to make a customized orbital floor implant. The advantages of using the SLS technique are that the objects made are cheap, easy and quick to make, have high precision, durability and are made of a versatile material. For this reason, other clinical requirements are satisfied. It allows precise primary reconstructions of orbital cavities, assuring the following advantages:

- Decrease of the surgical time and patient morbidity;
- Decrease of the surgery cost;
- Fast preoperative planning procedure.

A problem in making the mould concerns the two pins. These pins have the task of giving stability to the structure. At the end of the manufacturing process, the edges were subject to breakage. To solve

this problem, the thickness of the pins has been increased by almost double. Another problem concerns the deformation of the titanium prosthesis. In this study, a titanium mesh prosthesis was chosen because it has high biocompability, is malleable, is easily adaptable to the shape of the orbital defect and is not osteoinductive and resorbable. This problem is due to the fact that when the prosthesis is deformed, by loosening the pressure on it, there will be an elastic return causing the prosthesis to not fully deform. This problem can be solved by inserting another box in the mould, opposite to the first, so that the prosthesis can be inserted in the axes of the two holes of the two boxes in such a way as to avoid elastic return.

Being sterilizable, the device is usable in the operating room. Having a simple geometry, it is easy to use and is ergonomic. The limit switch device provides the surgeon with correct feedback for the correct positioning and orientation of the custom-made implant. The spring allows the device to hook and unhook the implant correctly. Being molded in polyamide, the device completely fulfills the requirement of low cost. Furthermore, the manufacture of a mould and the device through the SLS technique allows to reduce the duration of the operation. A first disadvantage of this device concerns its usability towards prostheses by deformation. In fact, in the case study, it was used with a titanium mesh prosthesis. No tests were performed to attach a demineralized bone plate. Another problem concerns the limit switch device. The latter, tracing the orbital edge of the case study, does not precisely provide correct feedback for the correct positioning of the custom-made implant. To solve this problem, another limit switch twice the size of the first has been designed to completely retrace the orbital edge. The last aspect to consider is tolerance. For both the mould and the medical device, we tried to make pins with a diameter slightly smaller than the holes of the custom-made implant. This has led to a tolerance problem in gripping the prosthesis with both the device and the mould. The solution is to have as tight a tolerance as possible so that you no longer have this problem. The purpose of this study was to create a device that is a valid alternative to the classic instruments on the market. To date, the operations for the restoration of the orbital floor can be performed with tracking devices. The latter have a high cost, require time to obtain a correct calibration and are not suitable for deformed prostheses. For this reason, this device has been designed in such a way as to eliminate problems related to cost, time, usability and that it is suitable for reconstructions of the orbital floor. Future research could solve the problem of using a demineralized bone plate or improve the limit switch device to have more feedback for the positioning of the prostheses.

7-REFERENCES

[1] D. J. Podolsky, J. G. Mainprize, G. P. Edwards, and O. M. Antonyshyn, "Patient-specific orbital implants: Development and implementation of technology for more accurate orbital reconstruction," *J. Craniofac. Surg.*, vol. 27, no. 1, pp. 131–133, 2016.

[2] S. Jank, R. Emshoff, B. Schuchter, H. Strobl, I. Brandlmaier, and B. Norer, "Orbital floor reconstruction with flexible Ethisorb patches: A retrospective long-term follow-up study," *Oral Surg. Oral Med. Oral Pathol. Oral Radiol. Endod.*, vol. 95, no. 1, pp. 16–22, 2003.

[3] M. B. Pritz and R. A. Burgett, "Spheno-orbital reconstruction after meningioma resection," *Skull Base*, vol. 19, no. 2, pp. 163–170, 2009.

[4] J. C. Carr, W. Richard Fright, and R. K. Beatson, "Surface interpolation with radial basis functions for medical imaging," *IEEE Trans. Med. Imaging*, vol. 16, no. 1, pp. 96–107, 1997.

[5] K. Moiduddin, A. Al-Ahmari, E. S. A. Nasr, M. Al Kindi, S. Ramalingam, and A. Kamrani, "Comparing 3-Dimensional Virtual Reconstruction methods in Customized Implants," *Int. J. Adv. Biotechnol. Res.*, vol. 7, no. 1, pp. 976–2612, 2016.

[6] G. Hayek, P. Mercier, and H. D. Fournier, "Anatomy of the orbit and its surgical approach.," *Adv. Tech. Stand. Neurosurg.*, vol. 31, pp. 35–71, 2006.

[7] C. René, "Update on orbital anatomy," *Eye*, vol. 20, no. 10, pp. 1119–1129, 2006.

[8] K. V. Slavin, M. Dujovny, G. Soeira, and J. I. Ausman, "Optic canal: Microanatomic study," *Skull Base Surg.*, vol. 4, no. 3, pp. 136–144, 1994.

[9] F. Govsa, G. Kayalioglu, M. Erturk, and T. Ozgur, "The superior orbital fissure and its contents," *Surg. Radiol. Anat.*, vol. 21, no. 3, pp. 181–185, 1999.

[10] T. A. Turvey and B. A. Golden, "Orbital Anatomy for the Surgeon," *Oral Maxillofac. Surg. Clin. North Am.*, vol. 24, no. 4, pp. 525–536, 2012.

[11] J. C. De Battista, L. A. Zimmer, P. V. Theodosopoulos, S. C. Froelich, and J. T. Keller, "Anatomy of the inferior orbital fissure: Implications for endoscopic cranial base surgery," *J. Neurol. Surgery, Part B Skull Base*, vol. 73, no. 2, pp. 132–138, 2013.

[12] J. M. Reyes *et al.*, "Classification and epidemiology of orbital fractures diagnosed by computed tomography," *Rev. Argentina Radiol.*, vol. 77, no. 2, pp. 139–145, 2013.

[13] U. V Thiagarajan B, "Blow Out Fracture Orbit Endoscopic Reduction a Novel Management Modality," *WebmedCentralENT Sch.*, vol. 3, no. 5, 2012.

[14] N. Romero, D. Lima, D. Luiz, G. Zorzetto, M. M. Capelari, and M. G. D. E. Oliveira, "Fracture of the Orbital Floor Type Blow-Out Literature Review * Fratura Do Assoalho Orbitário Tipo Blow-Out," no. July 2016, pp. 1417–1439, 2012.

[15] J. Leibsohn, "Orbital floor fractures," *Ophthalmic Semin.*, vol. 1, no. 4, pp. 451–514, 1976.

[16] J. W. Shin, J. S. Lim, G. Yoo, and J. H. Byeon, “An analysis of pure blowout fractures and associated ocular symptoms,” *J. Craniofac. Surg.*, vol. 24, no. 3, pp. 703–707, 2013.

[17] J. M. Joseph and I. P. Glava, “Orbital fractures: A review,” *Clin. Ophthalmol.*, vol. 5, no. 1, pp. 95–100, 2011.

[18] U. Vignesh, D. Mehrotra, Dichen, V. Anand, and D. Howlader, “Three dimensional reconstruction of late post traumatic orbital wall defects by customized implants using CAD-CAM, 3D stereolithographic models: A case report,” *J. Oral Biol. Craniofacial Res.*, vol. 7, no. 3, pp. 212–218, 2017.

[19] E. Ellis and Y. Tan, “Assessment of internal orbital reconstructions for pure blowout fractures: Cranial bone grafts versus titanium mesh,” *J. Oral Maxillofac. Surg.*, vol. 61, no. 4, pp. 442–453, 2003.

[20] S. Kang *et al.*, “Generation of customized orbital implant templates using 3-dimensional printing for orbital wall reconstruction,” *Eye*, vol. 32, no. 12, pp. 1864–1870, 2018.

[21] M. Mandolini, A. Brunzini, M. Germani, S. Manieri, A. Mazzoli, and M. Pagnoni, “Selective laser sintered mould for orbital cavity reconstruction,” *Rapid Prototyp. J.*, vol. 25, no. 1, pp. 95–103, 2019.

[22] I. R. P. Sunderland, G. Edwards, J. Mainprize, and O. Antonyshyn, “A technique for intraoperative creation of patient-specific titanium mesh implants,” *Can. J. Plast. Surg.*, vol. 23, no. 2, pp. 95–99, 2015.

[23] C. Lee Ventola, “Medical applications for 3D printing: Current and projected uses,” *P T*, vol. 39, no. 10, pp. 704–711, 2014.

[24] R. Petzold, H. F. Zeilhofer, and W. A. Kalender, “Rapid prototyping technology in medicine - Basics and applications,” *Comput. Med. Imaging Graph.*, vol. 23, no. 5, pp. 277–284, 1999.

[25] M. Attaran, “The rise of 3-D printing: The advantages of additive manufacturing over traditional manufacturing,” *Bus. Horiz.*, vol. 60, no. 5, pp. 677–688, 2017.

[26] S. F. Mustafa, P. L. Evans, A. Bocca, D. W. Patton, A. W. Sugar, and P. W. Baxter, “Customized titanium reconstruction of post-traumatic orbital wall defects: A review of 22 cases,” *Int. J. Oral Maxillofac. Surg.*, vol. 40, no. 12, pp. 1357–1362, 2011.

[27] O. Lieger, R. Richards, M. Liu, and T. Lloyd, “Computer-assisted design and manufacture of implants in the late reconstruction of extensive orbital fractures,” *Arch. Facial Plast. Surg.*, vol. 12, no. 3, pp. 186–191, 2010.

[28] M. Pagnoni *et al.*, “Late treatment of orbital fractures: a new analysis for surgical planning.,” *Acta Otorhinolaryngol. Ital.*, vol. 34, no. 6, pp. 439–45, 2014.

[29] E. B. Strong, S. C. Fuller, D. F. Wiley, J. Zumbansen, M. D. Wilson, and M. C. Metzger,

"Preformed vs intraoperative bending of titanium mesh for orbital reconstruction," *Otolaryngol. - Head Neck Surg. (United States)*, vol. 149, no. 1, pp. 60–66, 2013.

[30] M. Gerressen, S. Gilleßen, D. Riediger, F. Hölzle, A. Modabber, and A. Ghassemi, "Radiologic and facial morphologic long-term results in treatment of orbital floor fracture with flexible absorbable alloplastic material," *J. Oral Maxillofac. Surg.*, vol. 70, no. 10, pp. 2375–2385, 2012.

[31] T. Gander *et al.*, "Patient specific implants (PSI) in reconstruction of orbital floor and wall fractures," *J. Cranio-Maxillofacial Surg.*, vol. 43, no. 1, pp. 126–130, 2015.

[32] I. Ono, H. Gunji, K. Suda, F. Kaneko, and K. Yago, "Orbital reconstruction with hydroxyapatite ceramic implants," *Scand. J. Plast. Reconstr. Surg. Hand Surg.*, vol. 28, no. 3, pp. 193–198, 1994.

[33] M. Al-anezi, H. Mahran, M. Alomaym, S. Albati, and M. Alharbi, "Role of Titanium Mesh as a Reconstruction Material for Orbital Floor Defects in Cases of Orbital Blowout Trauma," *Ohdm*, vol. 17, no. 5, pp. 1–5, 2018.

[34] G. Ramieri, M. C. Spada, S. D. Bianchi, and S. Berrone, "Dimensions and volumes of the orbit and orbital fat in posttraumatic enophthalmos," *Dentomaxillofacial Radiol.*, vol. 29, no. 5, pp. 302–311, 2000.

[35] D. E. E. Holck, E. M. Boyd, J. Ng, and R. O. Mauffray, "Benefits of stereolithography in orbital reconstruction," *Ophthalmology*, vol. 106, no. 6, pp. 1214–1218, 1999.

[36] J. Hoffmann, C. P. Cornelius, M. Groten, L. Pröbster, C. Pfannenberg, and N. Schwenzer, "Orbital reconstruction with individually copy-milled ceramic implants," *Plastic and Reconstructive Surgery*, vol. 101, no. 3. pp. 604–612, 1998.

[37] A. W. Sugar, M. Kurlakose, and N. D. Walshaw, "Titanium mesh in orbital wall reconstruction," *Int. J. Oral Maxillofac. Surg.*, vol. 21, no. 3, pp. 140–144, 1992.

[38] E. A. Mohamed, S. A. Hassan, R. M. Kamel, F. Mohamed, and Shadia A. Elsayed, "Orbital Defect Reconstruction: the Use of Preformed Titanium Plates Versus Custom-Made Titanium Computer Assisted Implants," *Al-Azhar Assiut Med. J.*, vol. 13, no. 4, pp. 262–275, 2015.

[39] L. Guo, W. Tian, F. Feng, J. Long, P. Li, and W. Tang, "Reconstruction of orbital floor fractures: Comparison of individual prefabricated titanium implants and calvarial bone grafts," *Ann. Plast. Surg.*, vol. 63, no. 6, pp. 624–631, 2009.

[40] D. C. Garibaldi, N. T. Iliff, M. P. Grant, and S. L. Merbs, "Use of porous polyethylene with embedded titanium in orbital reconstruction: A review of 106 patients," *Ophthal. Plast. Reconstr. Surg.*, vol. 23, no. 6, pp. 439–444, 2007.

[41] M. Vehmeijer, M. van Eijnatten, N. Liberton, and J. Wolff, "A Novel Method of Orbital Floor

Reconstruction Using Virtual Planning, 3-Dimensional Printing, and Autologous Bone," *J. Oral Maxillofac. Surg.*, vol. 74, no. 8, pp. 1608–1612, 2016.

[42] A. Mazzoli, "Selective laser sintering in biomedical engineering," *Med. Biol. Eng. Comput.*, vol. 51, no. 3, pp. 245–256, 2013.

[43] E. Maravelakis, K. David, A. Antoniadis, A. Manios, N. Bilalis, and Y. Papaharilaou, "Reverse engineering techniques for cranioplasty: A case study," *J. Med. Eng. Technol.*, vol. 32, no. 2, pp. 115–121, 2008.